LONDON, METEOROLOGICAL OFFICE.

Met.O.16 Branch Memorandum No.6.

An experimental study of the remote location of lightning flashes using a VLF arrival time difference technique. By LEE, A.C.L.

London, Met.Off., Met.O.16 Branch Mem.No.6, 1985, 31cm. Pp.71, 7 pls. 26 Refs. Abs.pp.1-2.

An unofficial document - restriction on first page to be observed.

Met O 16 BRANCH MEMORANDUM No. 6.

AN EXPERIMENTAL STUDY OF THE REMOTE LOCATION OF LIGHTNING FLASHES USING A VLF ARRIVAL TIME DIFFERENCE TECHNIQUE

by

Anthony C. L. Lee

An experimental study of the remote location of lightning flashes using a VLF arrival time difference technique

By A.C.L.LEE

Meteorological Office, Bracknell

SUMMARY

The potential of an "Arrival Time Difference"(ATD) technique for replacing the operational "Cathode Ray Direction Finding"(CRDF) network for the location of lightning flashes at ranges of up to thousands of kilometers is discussed. The ATD technique has theoretical advantages over CRDF, which could lead to substantially improved flash location, but the extent to which it suffers from certain propagation effects in practice must be quantified.

An experimental study of the ATD technique is presented, based on the deployment of equipment in the UK and Gibralter. These equipments are used to capture the vertical electric field of VLF electromagnetic radiation from individual lightning flashes, synchronised to signals captured by the CRDF system. The resulting waveform data are recorded against an accurate timebase. By analysing the data using techniques analagous to those of hyperbolic navigation,

the flash location can be inferred, together with a measure of the consistency of the data.

The results are compared with the CRDF and other meteorological data, and appear to agree to within the limited accuracy of the current techniques.

An analysis method is developed which relates the internal consistency of the ATD flash data to geographical location accuracy. On this basis, the accuracy of an operational ATD system could exceed that of the CRDF system by an order of magnitude or more.

1. INTRODUCTION

For the past forty years the Meteorological Office has operated the so-called "Sferics" system for locating lightning flashes at ranges of up to around 3000 km by making measurements on the radio atmospheric, or "Sferic", associated with the lightning discharge in the Very Low Frequency or VLF band. The operational system is based on the Cathode Ray Direction Finding, or CRDF, principle (Ockenden, 1947; Adcock and Clarke, 1947; Maidens, 1953; Horner, 1954(a)). This paper describes some results of a

Trial which took place during 1978 and 1979 on an alternative "Arrival Time Difference" or ATD principle for flash location which was considered more suitable for a highly automated replacement for the obsolescent and labour intensive CRDF system.

2. THE "CRDF" SFERICS SYSTEM

(a) Basic CRDF flash location

In the existing operational system, the Sferic associated with a lightning discharge is received at around seven Outstations. These are direction-finding receivers located at sites spread over the United Kingdom and the Mediterranean, each linked to a plotting station at Beaufort Park, near Bracknell, UK. Each Outstation (Horner, 1954(a)) comprises a pair of crossed loop antennae, with suitably matched signal amplifiers and filters for each antenna. The Sferic signals are amplified and filtered before being applied to the X and Y deflection plates of a precision cathode-ray tube (CRT), to draw a line on the CRT whose orientation is a measure of the apparent bearing from the Outstation to the lightning flash with which the Sferic was associated. An Outstation operator, hearing a centrally-generated synchronising signal, measures the orientation of the corresponding line from the CRT's

afterglow, and reports it to Beaufort Park. Here, the Outstations' reports on each selected lightning flash are plotted, and a location, or "fix", obtained by triangulation on a gnomonic projection which maps bearings (great circles) into straight lines (Keen, 1938).

This simplified over-view is the essence of the so-called cathode-ray direction-finding or CRDF system, whose output is reported internationally as "SFLOC" messages on the WMO global telecommunication system.

(b) Propagation effects

The CRDF system utilises Sferic signals in a bandwidth of around 250 Hz, centred on a frequency of 9 kHz; approximately where the spectrum of the emitted radio-wave energy peaks (Arnold and Pierce, 1964; Alpert et alia, 1967). At these VLF wavelengths of around 33 km, an impulsive "ground-wave" ray diffracts around the curved surface of the earth, and a "sky-wave" ray reflects - with some dispersion - from the conducting ionosphere at a height of 70-90 km. A returning sky-wave will reflect from the conducting earth. Thus a receiver at some distance from the original flash will receive a ground-wave, followed by the first sky-wave (one ionospheric reflection), followed by a second sky-wave (ionosphere, ground, ionosphere) and so on (Schonland et

alia, 1940; Wait, 1961). The time-separation of the successive sky-waves is of the order of 50-200 μs, and is caused by the increased path-length travelled. The practical duration of this earth-ionosphere waveguide impulse-response is of the order of 200-500 μs as the highest order sky-waves become rapidly attenuated (Alpert et alia, 1967). However, in any experimentally monitored Sferic signal this detailed structure is convolved with the Sferic source field (of significant duration 50-100 μs for a return stroke, extending to several ms for complicated charge movements) which causes overlap of the successive sky-waves; and then with the impulse response of the detection equipment filters, to form a complex waveform. With adequately wide equipment filter bandwidths, the complexities of charge movements through the tortuous paths of a lightning discharge ensure that Sferic waveforms vary quite widely in shape, giving each a unique signature (see Norinder, 1954, for examples).

The Sferic radio-wave energy is thus trapped inside the wave-guide formed from the conducting earth and ionosphere, and spreads two-dimensionally rather than three-dimensionally. In addition to this relatively small spreading loss, there is an energy loss through absorption, although this amounts to a mere 1-3 dB per Mm for frequencies near 9-10 kHz (Chapman et alia, 1966). These two factors combine to ensure that Sferic signals at these frequencies can be received over vast distances. Clearly there is potential for a system exhibiting enormous range, although

there is a corollory that the limiting factor in detecting weak Sferics of nearby origin is the permanent presence of a background of Sferics from distant intense sources, such as the equatorial regions.

Further background is given in Watt(1967), whose discussion concentrates on sinusoidal transmissions. Horner(1964) relates more directly to Sferics.

(c) Limitations in CRDF flash location

In practice the CRDF system cannot locate flashes accurately at extreme range because errors in the bearing measurements, combined with a baseline constrained by politics and communications costs, limit the accuracy with which their positions can be estimated by triangulation.

The prime cause of bearing error for relatively large, isolated Sferics lies in the implicit assumption of the crossed-loop direction-finder that the signal is vertically polarised, implying that the horizontal magnetic field component is perpendicular to the propagation path. In practice the effects of partial horizontal polarisation at source (Yamashita and Sao,1974(a)), the interaction of the Sferic signal with free ionospheric electrons in the presence of the earth's magnetic field (Yamashita and Sao,1974(b)), and the effects of non-horizontal conducting topography near the receiver site (Horner, 1954(b)), each contribute a

vertical magnetic field component in the Sferic signal. Where the received Sferic ray has an appreciable angle of elevation, which is certainly true for reception of sky-wave signals, this vertical magnetic component is tilted to produce a horizontal magnetic field in the direction of the propagation path. This "abnormal" component induces a voltage in the crossed-loop antennae giving rise to a "polarisation" error in bearing (Keene, 1938). The magnitude of this effect is of the order of 1-2° by day, and 10° or so by night (Horner, 1954 (b)).

For smaller amplitude Sferics, relatively more frequent, interference by overlapping Sferics can be a source of error; this may become dominant for Sferics at ranges beyond 1500 km (Horner, 1954(b)).

Very large bearing errors can be introduced by the presence of buried conductors at the receiver site, although it may be possible to eliminate the effect (Horner, 1953).

Finally, the limited time discrimination of the human operator is important. Under active thunderstorm conditions when Sferics of significant amplitude occur frequently, the operator may be unable to decide which of two or more lines drawn nearly simultaneously on his screen (although not corresponding to "overlapping" Sferics) correspond to the audio synchronising signals triggered by receipt of a particular Sferic at one of the Outstations. In this case there is a very real possibility of reporting the bearing of

the wrong Sferic. Undetected errors of this type certainly degrade the performance of the present CRDF system.

3. THE "ATD" SFERICS SYSTEM

(a) Basic ATD flash location

The earth-ionosphere waveguide gives a Sferics detection system operating near 9-10 kHz the potential for enormous range, but the magnitude of polarisation errors mean that this potential cannot be realised through CRDF unless uneconomically large base-lines are used. This dilemma leads to a search for alternative techniques which avoid the polarisation difficulty.

A promising approach is the Arrival Time Difference (ATD) technique. If a Sferic is received from a flash at two geographically separated Outstations, the difference in arrival times of the Sferic at each of the Outstations defines a locus of constant time-difference through the location of the flash . If a third separated Outstation exists, then a second locus may be inferred from the ATD between it and one of the original pair. The intersection of the loci defines a fix. Signal polarisation has no direct effect in this technique.

A set of three Outstations gives two legitimate fixes on a spheroidal earth. Adding a fourth Outstation gives a unique fix for error-free ATD values, and as the correct fix is over-determined one can obtain a measure of the internal consistency of the estimate of this fix when measurement errors exist (eg by comparing the three "correct" fixes obtained by taking Outstations three at a time). In practice, it is always necessary to design an Outstation network with considerably more than four Outstations to avoid having regions where the fix is unduly sensitive to small measurement errors, and to be able to cope with technical problems at some of the Outstations. In this case the fix is obtained through a maximum likelihood estimate based on the available measurement data and its likely errors (Appendix D).

The effects of network geometry can be made intuitively obvious by considering the loci of constant time-difference for a pair of Outstations. Along the base-line between the Outstations, these loci are uniformly spaced by 150m/μs, implying a uniformly high resolution in this direction. In the regions adjacent to the base-line, the uniformly spaced parallel loci diverge into curves initially resembling a family of hyperbolae with the Outstations as foci; thus the spacial resolution perpendicular to these curves decreases with range. (At extended ranges the "hyperbolae" actually form closed curves round the earth). As the base-line is followed into the "base-line extention" beyond either

Outstation, the ATD is independent of position, giving an indeterminate contribution by this locus to a fix. In a network exhibiting poor geometry, the effects of the base-line extention are clearly visible in charts of predicted accuracy.

To effect a fix, a second locus derived from a third Outstation is necessary. Under ideal geometrical conditions, the loci may intersect orthogonally in a region of 150 m/μs along both axis; an ATD accuracy of, say, 25 μs then gives a fix accuracy of 5.3 km. With more Outstations this can be improved statistically, but the geometry is likely to be less favourable, giving scant improvement.

At the edge of the useable service area loci may intersect at a narrow angle, giving a fix whose accuracy lacks directional symmetry. Thus from a compact distribution of Outstations the "bearing" of a distant fix may be accurate, but its range may be uncertain. This paper makes no attempt to quantify directional symmetry, but merely predicts system accuracy by calculating the RMS distance between "true" flash position and estimated "fixes" using Monte Carlo techniques for assumed levels of timing error.

(b) Extraction of the arrival time difference

Computer simulation of flash location estimation using realistic numbers of Outstations at feasible sites indicates that adequate accuracy for a CRDF system replacement would be obtained if ATD errors of the order of 25 μs could be achieved, although the differences between the systems makes a precise intercomparison difficult. If Outstations become unavailable for short periods because of technical problems, then considerably higher precision in ATD becomes valuable. If the time to correct such unavailability can be extended, this can reduce maintenance costs dramtically, but at the expense of the need for yet more precision in ATD.

From the description of Sferic propagation given above, it is clear that a Sferic signal has a duration considerably in excess of 25 μs, so there may be difficulties in assigning a unique epoch to its reception. To overcome this problem, a correlation technique was developed (Appendix C) for aligning Sferic waveforms received at different sites, and obtaining the ATD corresponding to the best match between pairs of waveform shapes. Thus for similar waveform shapes an accurate ATD can be obtained without the need to identify particular features on any waveform. Because bearings are not required, an omnidirectional vertical whip or similar electric field antenna can be used, and the state of polarisation of the received wave becomes essentially irrelevant.

The correlation technique is not a panacea. The description of the propagation mechanism given above indicates how the time separation between the reception of a ground-wave and successive sky-waves can be calculated from a simple geometrical model of ray propagation by considering the longer path lengths for the higher order sky-waves. If the distance between the flash and the receiver is increased, this model shows how the differences in path lengths are reduced, so that the sky-waves appear to "catch up" with the ground-wave and the phase structure of the Sferic becomes compressed towards the ground-wave. In addition, more complicated models show how the relative amplitudes of the various ground/sky-waves change. The ground-wave can only propagate by diffraction, and so becomes rapidly attenuated. The sky-wave amplitude depends on the ionospheric reflection coefficient which varies with angle of incidence (Wait and Walters, 1963), and also on ground reflectivity which varies from land to sea paths. This is a grossly over-simplified discussion, but it does indicate that the shape of the received signal varies with the propagation path, causing potential difficulties for a simple waveform-matching technique.

These propagation effects do not, however, necessarily invalidate the technique. For the more distant flashes the greatest precision in measuring ATD is necessary to achieve adequate geographical accuracy. Fortunately, the extreme range of these flashes implies that the propagation path is likely to be similar for both the Outstations involved in

estimating an ATD, implying a similarity between the waveforms. This similarity implies an accurate ATD estimate, alleviating the unfavourable geometry, and giving an acceptable fix. A hidden advantage of the correlation technique with such similar waveforms is its correspondence to a matched-filter technique. This gives the maximum possible signal-to-noise ratio for signals corrupted by additive noise (eg Schwartz, 1970), and helps to discriminate against any interfering Sferics of different signature; an important consideration for the more distant flashes which may be relatively weaker and more subject to additive interference.

The flashes of closer origin do not enjoy these advantages to the same extent, but a higher tolerance is allowable on the measurement of ATD to achieve an adequate fix. Where propagation path lengths differ considerably, the different compression effects can be sufficiently pronounced for the correlation technique to match waveforms a whole cycle (approx 100 μs) in error. Fortunately, using the correct technique (Appendix C) the possibility of this error can be made evident; and in the differentiated path-length situations where it does occur, errors as large as 100 μs still give acceptable fixes.

If greater location accuracy is necessary, there exists the theoretical possibility of applying a crude propagation correction (e.g. wave-hop model; Watt, 1967) to reduce the differential waveform shape, although this increases the

processing resources required.

(c) Site effects

In the CRDF system the polarisation (and hence the bearing error) of received Sferics is strongly influenced by local "site" effects such as local terrain topography, and the presence of local conducting wires, fences etc. In adddition, the site error or its correction is influenced by errors in the azimuth and even elevation angles of the antennae themselves. As a result, a potential CRDF site has to be chosen with great care, and may thus be expensive. Operation in a cramped site, in rugged terrain, or at sea is generally unlikely to be successful.

The ATD system uses an omni-directional vertical whip antenna for receiving Sferics signals, thus eliminating potential azimuth effects. Actual "site" effects are difficult to envisage as the state of polarisation of the received Sferic is not directly relevant, only its detected waveform. Antenna shielding reduces antenna sensitivity, but leaves waveform unaffected. To modify the received phase of a Sferic one might imagine a Sferic waveform received directly, and also received after reflection from some structure. If the sum of the waves is to have a noticeably different shape from the direct signal, there must

be a significant fraction of a wavelength (33 km) between the structure and the antenna. At this separation, the structure would need to be near resonance to contribute significant reflected amplitude implying a vertical quarter-wave conducting structure 8 km high. This seems unlikely, so that the effects of "site" errors are probably negligible.

(d) An early measurement

Lewis, Harvey and Rasmussen (1960) attempted to "locate" lightning flashes in the UK using a pair of ATD stations at two sites in the USA spaced 139.4 km apart near New England.

They selected flashes by receiving the CRDF synchronising signal, so that some of their data corresponded to UK flashes for which a CRDF location estimate was available. Their stations each consisted of a wideband (4-45 kHz) receiver with a vertical whip antenna, connected via a suitable microwave link to a central location where signals were recorded automatically on 35 mm film, together with suitable timing marks. Time difference extraction was achieved by matching waveforms visually, taking care to obtain a detailed match near the early waveform peaks.

With just two stations an actual fix cannot be obtained, but one may compute the perpendicular vector between the locus of constant time difference for the measured ATD, and the "known" CRDF location estimate. Their result showed a negligibly small mean bias of 0.6 km south, with a standard deviation of 57 km. This agreement in the placing of a locus to 57 km from a range of 5600 km is especially remarkable because of the likely errors of the CRDF networks. The 57 km standard deviation corresponds to a standard deviation in bearing of 0.6 degrees, or in ATD of 4 μs.

Their result does not indicate directly how a network might perform, as this depends on network geometry which might be unfavourable. However, it is clear that ATD might be measured to better than 4 μs, at least for flashes at a range of 5600 km which are nearly equi-distant from two receivers spaced by 139.4 km, and hence show nearly identical propagation effects. This gives clear encouragement for a long-range network which demands ATD accuracy of 25 μs, but provides little evidence on how a more realistically spaced network might respond to flashes of shorter range.

4. THE SFERICS TRIAL TECHNIQUES

(a) Introduction

In early 1977 an ATD Sferics Trial comprising four Outstations, the minimum number for reliable fixing, was mounted. The equipment and techniques used are described here partly as the Trial record, and partly because the future Meteorological Office operational ATD system has been designed on comparable lines.

(b) Waveform processing

Fig 1 illustrates a Sferics Trial Outstation. The vertical electric field of any Sferic disturbances are capacitively coupled to a vertical whip antenna, inducing currents into a virtual earth. The Sferics Sensor electronics include an integrator, so that the Sensor output is related to vertical electric field input by a constant gain over an adequate frequency range from tens of Hz to around 1 MHz.

The Sensor signal passes into the Sferics Filter. This is largely a broad band-pass filter which dominates the

system's response to any impulsive signal (Appendix A) exhibiting 3 dB attenuation limits at 2 kHz; and 50 dB attenuation at 50 kHz, for anti-alias properties. The Sferics Filter also contains a gain control, and a number of highly stable narrow band-reject "notch" filters of width 100 Hz designed to remove the unwanted effects of man-made transmitters operating within the frequencies of interest. Fortunately, from our point of view, it is difficult to design an efficient wide-band transmitter antenna to operate at these wavelengths, so that narrow notch filters can be used to minimise Sferic distortion (Appendix A).

The analogue waveform then passes into a Transient Recorder where it is digitised to 256 equally spaced levels at accurately spaced intervals of 10 μs, giving a Nyquist frequency of 50 kHz. The Transient Recorder normally samples continuously, and retains the last 1024 samples or 10.24 ms of data. On receipt of a digital signal from the Timing Interface (initiated by receipt of a Sferic signal), the Transient Recorder continues for 512 samples and then stops, thus freezing the signal of interest near the centre of a 10.24 ms data window.

(c) Synchronisation to CRDF

The analogue waveform from the Sferics Sensor is also

presented to a "Narrow Band" filter which has the characteristics of the CRDF filters, and thus responds similarly to Sferics. Its output drives a Threshold device which generates a digital output for waveforms of sufficient amplitude. The operator adjusts the Threshold Gain until the Threshold device responds to the same Sferics as the CRDF system. The digital signal is presented to a Timing Interface which freezes the Transient Recorder as described above, and also latches the display of a "Local Timescale" formed from a precision (Rubidium) 10 MHz Oscillator and a continuously accumulating Counter.

The Timing Interface normally freezes the Transient Recorder and Counter display for a period of one second only before normal continuous digitisation and Counter display are resumed. However, should the operator receive a CRDF synchronising signal, during the one-second period he can direct the Timing Interface to "hold" the frozen data, and transfer it to a Magnetic Logger for later analysis. Thus the Trial Outstation can capture Sferics from flashes selected by the CRDF system, contained within an adequate data window of 10.24 ms, together with Local Timescale epoch data recording the instant of a particular sample of the waveform.

(d) Potential ATD resolution

The analogue waveform presented to the Transient Recorder is sampled and stored every 10.00 μs. Shannon (1949) showed that a sampled waveform of infinite duration contains all the information necessary to reconstruct the original underlying continuous waveform, provided that the original continuous waveform contained no energy above the Nyquist frequency limit of one cycle per two samples: 50 kHz in this case. The present signal is both finite and imperfectly band limited. However, to within the resolution of an 8-bit quantiser, the sampled waveform is a complete and accurate representation of the original continuous waveform (Appendix B). Thus one may conceive of matching two similar "continuous" waveforms to extract time-differences with a resolution of the order of 0.1 μs, in spite of the fact that the samples are 10 μs apart.

(e) Spectral calibration and correction

To measure time-differences to 0.1 μs from frequencies of the order of 10 kHz, it is evident that the analogue filters used must be characterised accurately. The approach taken here is to generate a highly reproducible known pseudo-noise analogue test signal on the Timing Interface, to present this

to the Sferics Filter instead of the Sferics Sensor output, and to trigger the Transient Recorder at a known phase of the pseudo-noise signal. Because the test signal is known, and the Transient Recorder's stored data is band-limited, this gives all the information necessary to evaluate the filter transfer function, and to calculate the "Deviation Spectrum" relating the measured spectrum to a mathematical ideal (Appendix B). This process is termed "Spectral Calibration", and was performed routinely throughout the Sferics Trial. When waveforms were subsequently received through the calibrated filters, the Deviation Spectrum was used to correct each waveform to the shape that would have been received through a mathematically correct filter - a process termed "Spectral Correction" (Appendix B). The act of Spectral Calibration not only allows the inevitable minor deviations of hardware filter profiles to be corrected, but also provides timely warning of any catastrophic problems.

A Spectral Calibration process was also performed by applying the pseudo-noise signal via a capacitor to an electrostatically shielded antenna; a functioning system should show little more than an increased Group Delay characteristic. This test was augmented by connecting an external three-ohm resistor from antenna to earth, which modifies the measured transfer function by a known amount, confirming that the antenna base "virtual earth" is within a few ohms of zero input impedance. A low input impedance ensures that damp-induced leakage conductance between antenna and earth, in parallel with the virtual earth, does not cause

subtle but significant phase distortion.

(f) Epoch calibration and correction

An immediate technical problem is the synchronisation and maintenance of local timescales at widely dispersed Outstations to an accuracy approaching 0.1 μs. The approach here was to take a precision 10 MHz (Rubidium) Oscillator, stabilise its environment to enhance the basic stability, and to monitor the phase offset against International Atomic Time as a function of time by various means. Most methods of monitoring phase offset are subject to periods without measurements, but a suitably stable oscillator can have measurements adequately interpolated (or predicted in an operational system). These measured offsets were not used to adjust the oscillator, but to correct the reported epoch values associated with waveform data. Corrupt monitoring measurements can then be identified and rejected.

The Rubidium oscillator was housed in a thermally insulated enclosure which stabilised the oscillator's thermal plate temperature to within a few hundredths of a degree Centigrade. In addition, the time integral of temperature was explicitly stabilised. Thus any external effects which caused the thermal plate temperature to fall, perhaps slowing

the local timescale, were compensated by a subsequent temporary rise to above nominal temperature. This had the effect of allowing the local timescale to catch up its lost phase before significant error could accumulate.

For the same reason, the supply voltage for the Rubidium Oscillator was stabilised, as was its time integral. Pressure is known to have an effect on the Rubidium oscillator, and was monitored.

A number of ways of estimating International Atomic Time were used, including a Loran-C Receiver, a VLF Receiver, an MSF Time-Code Receiver, and a travelling Atomic Clock. Each provided a regular digital square wave having a "known" epoch for one edge, and an "ambiguity" equal to the square-wave period. These were presented to the Timing Interface, and the local timescale epoch for the significant edge measured and recorded. By taking the measured epoch modulo the ambiguity, a residual was obtained whose variation with time gave the modulo relative time shift between the local timescale and that particular estimate of International Atomic Time. In general the variation was sufficiently slow to be plotted to a resolution of 0.1 μs, and interpreted manually.

All these International Atomic Timescale estimates had their own advantages and drawbacks:

i. Loran-C was the most precise, although the method

needs a complex and (at some sites) difficult setting-up procedure, is subject to ambiguities through potential operator error, and to around 0.3 μs uncertainty in predicted propagation delay. Should the receiver lose track of the Loran-C transmission for any reason, the manual setting-up procedure must be repeated. However, the method is excellent for determing drift in the local timescale, and a fair degree of accuracy can be obtained in absolute epoch if the potential ambiguities can be resolved.

ii. The VLF Receiver was essentially a narrow-band phase-locked loop for phase-stabilised VLF carriers such as GBR, Rugby. The simplicity of the technique meant that automatic "lock-on" was easily achieved, but because a variable mixture of ground wave and sky-waves from an ionosphere of varying height was received, the measured phase suffered a marked diurnal variation, was subject to ionospheric disturbance, and even during the most stable (mid-day) period was uncertain in phase to within around 2 μs or more depending on the transmission path used.

iii. The MSF Receiver was useful for resolving large ambiguities in other methods, but had insufficient accuracy to be useful in isolation.

iv. The Travelling Atomic Clock (portable battery-supported Rubidium Oscillator) was calibrated at the National Physical Laboratory, transported to the

Outstation site where local timescale measurements were made, and then transported back to the National Physical Laboratory for re-calibration. While the Travelling Atomic Clock was away from a calibrated standard, its own calibration would slowly drift because of inherent deficiencies in the oscillator; and because of the changes in environment, standby battery state, etc. After each round trip, the calibration had drifted by several microseconds. However, the impact of this was considerably reduced by monitoring its drift against Loran-C while stationed at the Outstation site, reducing the drift to that experienced during actual travel. In this way the uncertainty of a Travelling Clock calibration was reduced to around 0.2 μs for most sites. Furthermore, if several calibrations obtained over a period of time could be compared through Loran-C, the uncertainty of an individual calibration can be reduced statistically. A series of Travelling Clock exercises can thus be used to determine an accurate propagation delay from Loran-C transmitters to the Outstation site. The Travelling Atomic Clock/Loran-C combination is thus a highly successful method of calibrating Loran-C epoch absolutely, and resolving the Loran-C ambiguities. However, the process of transporting an unwieldy Travelling Atomic Clock is expensive, frustrating, and is subject to the very real risk of physcial damage to the clock, or losing epoch through transport delays exhausting the Travelling Clock's internal batteries.

(g) ATD extraction and flash fixing

The ATD between waveforms received at different Outstations was estimated by correlating the 10.24 ms data windows, and selecting the time-difference for the highest correlogram peak (Appendix C).

A problem arises when an interfering Sferic is received at an Outstation at nearly the same time as a "wanted" Sferic (which was received at the other Outstations). For the trial, the distance between the Reference Outstation at Beaufort Park (Appendix C) and the furthest Outstation was 1731 km, corresponding to a maximum possible ATD of 5.8 ms. Thus selected interfering Sferics producing a larger ATD need generate no misleading results - merely the nuisance of lost data.

When the interfering and wanted ATD values are close, the two Sferics will nearly always be visible within the 10.24 ms data window. The correlation technique estimates the smilarity in shape between the waveforms in the two data windows (signal-to-noise ratio, Appendix C) which is reduced if two waveforms are present, indicating an unreliable ATD.

If the wanted Sferic is outside the data window surrounding the interfering Sferic, the ATD error is likely to be large enough to imply an abnormally large flash location RESIDUAL (Appendix D), indicating an unreliable fix.

Any techniques which increase the signal-to-noise ratio and reduce RESIDUAL will increase confidence that misleading flash data will be rejected, as well as increase fix accuracy. Possible methods include the use of a carefully chosen "conditioning filter" profile (Appendix B), correction of waveform shapes for differential propagation effects via an iterative technique, maintenance of adequate standards of epoch calibration and correction, and realistic theoretical ATD models (Appendix D).

5. TRIAL RESULTS

(a) The trial geometry

Between October 1978 and October 1979, Sferics waveform and epoch data were collected during six periods of approximately ten days, synchronised to CRDF operation, under day and night conditions; four periods produced results suitable for analysis.

During these periods the experimental ATD Outstations were located as shown in Fig. 2, at Shanwell (56.439°N, 2.862°W), Camborne (50.218°N, 5.326°W), Beaufort Park (51.390°N, 0.784°W), and Gibraltar (36.155°N, 5.340°W). The CRDF stations were located at Lerwick (60.14°N, 1.18°W), Shanwell, Camborne, Hemsby (52.69°N, 1.69°E), Gibraltar, and Malta (35.90°N, 15.40°E), also shown in Fig. 2, in a much more satisfactory geographical distribution.

Fig. 2 is a gnomonic projection with a tangential point at 43.0°N, 12.0°E. The contours display a geometrical progression of expected RMS error in ATD flash location; units are kilometres. These were calculated as above using a Monte-Carlo method assuming the experimental ATD network and a Gaussian distribution of ATD errors, standard deviation 25 μs, with Beaufort Park as the Reference Station. The effects of the base-line extensions are clearly visible. This serves as a theoretical comparison for the trial results

presented below. An operational network would use a better geographical distribution of Outstations to achieve an improved service area. Fig. 3 shows the expected location error in RMS km for a possible network of seven Outstations calculated in the same way for the same distribution of ATD errors, but with the Reference Station at Aughton (53.55°N, 2.55°W). An accuracy of well under 100 km for the assumed 25 μs ATD error is maintained over the chart shown, representing a considerable improvement over a seven-station CRDF network including Outstations at Gibraltar, Malta and Cyprus (Meteorological Office, 1975).

(b) Problems in direct CRDF/ATD comparison

A trial aim was to locate individual flashes by both the established CRDF system and the experimental ATD system, to permit a direct comparison of their fixes. Using the same map projection as that of Fig. 2, the corresponding CRDF (+) and ATD fixes were plotted joined by a line as shown in Figs. 4 and 5. The gnomonic projection allows bearings from the CRDF stations to be interpreted easily, while the chosen tangential point ensures that distance scaling is almost uniform in the areas shown.

This analysis has difficulties. An ATD fix is necessary, implying that data for corresponding Sferics are required from all four ATD Outstations. Because of the "freeze" time inherent in the trial ATD Outstation design, only 10% of ATD

recorded flashes qualify, reducing the useful data available.

Conversly, for each suitable ATD fix a corresponding CRDF fix is required. The technique for timing CRDF selected flashes had a resolution of 2-3 seconds, and two or more unresolved Sferics frequently occurred above threshold during such an interval. The ATD system would select the earliest, while the CRDF operators might select the largest as viewed on the cathode-ray tube after-glow. Thus the systems could fix different flashes. Alternatively, the CRDF operators might select different flashes at different Outstations, thus not providing enough bearings on the same flash to establish a fix. This further reduces the data available.

The latter CRDF problem is well known. It leads to lost data if a storm has only a single flash selected; but storms usually generate many flashes, and several may be selected. Thus CRDF plotting operators examine the sets of bearings obtained during a 10-minute observation period, and assume that similar sets correspond to the same storm location. To achieve "similar" sets, they may discard bearings from each that appear to correspond to unrelated flashes. Although individual flashes may now contribute few bearings, a "composite" fix is estimated from many flashes using an average of the selected bearings from each CRDF Outstation. Thus apparent CRDF fix consistency is not significant, it merely indicates a composite fix assigned to each of its member flashes. The corresponding ATD fixes are independent.

(c) Direct CRDF/ATD comparisons

(i) A Winter comparison. Fig. 4 displays the 41 four-station ATD fixes associated with CRDF fixes that occurred within the displayed region on 26 November 1978 between 1520 - 1700 hrs GMT. The ATD fixes are each shown joined by a straight line to the associated CRDF fix (+) on the same gnomonic projection as Figs. 2, 3. The data were selected for display on the basis of being quite typical, and of highlighting certain features observable in all the trials data. Fig. 4 gives a good visual impression of the spatial relationships of the flash data and geography. The synoptic situation was that of a deepening low centered to the north-west of Corsica, with thunderstorm observations reported in this area.

Table 1 gives tabulated location data for these 41 flashes, which are arranged in groups corresponding to the same composite CRDF fix. As well as providing greater resolution, Table 1 details the time of the flash and the quantity RESIDUAL - discussed below - whose small values indicate that all these ATD fixes are internally self-consistent. In addition, Table 1 details the site-corrected CRDF bearing measurements used to estimate the CRDF fixes, and for comparison the calculated ellipsoidal-earth bearing of the ATD fix from each of the

TABLE 1 – COMPARISON OF CRDF AND ATD FLASH DATA: CRIF GROUPING

FLASH IDENTIFICATION NUMBER	FLASH LOCATION				TIME OF FLASH (GMT)	ATD RESID	BEARINGS FROM EACH CRDF STATION TO A FLASH FIX									
	CRDF FIX		ATD FIX				CAMBORNE		SHANWELL		HEMSBY		LERWICK		MALTA	
	°N	°E	°N	°E	HH MM SS	μS	CRDF	ATD	CRDF	ATD	CRDF	ATD	CRDF	ATD	CRDF	ATD
2045	43.0	11.0	41.646	11.972	15 21 13	2.09	118	118.90	144	140.72	141	143.76	146	150.41	163	156.03
2075	"	"	43.601	7.891	15 28 17	0.93	120	121.17	146	147.37	152	153.17	–	157.54	150	145.38
2047	37.9	4.9	38.302	5.077	15 21 27	0.26	145	144.12	170	160.39	170	169.37	163	166.88	111	109.27
2086	"	"	38.311	3.999	15 30 36	1.68	148	147.26	170	162.95	173	172.72	163	169.11	113	108.19
2053	38.6	17.4	38.361	8.808	15 22 48	0.12	143	134.26	–	151.82	157	158.16	154	159.29	123	116.96
2082	"	"	38.363	8.855	15 29 34	1.20	143	134.14	–	151.71	159	158.02	155	159.20	129	117.13
2054	39.9	3.0	40.126	3.124	15 22 59	0.31	150	146.27	170	163.92	176	174.96	163	170.40	121	117.22
2058	"	"	38.078	5.188	15 23 28	0.59	150	144.24	169	160.29	169	169.16	160	166.74	117	107.93
2055	35.7	3.3	36.518	2.355	15 23 07	0.79	156	155.02	176	167.77	181	178.07	166	172.90	98	97.19
2064	"	"	36.761	3.232	15 25 27	1.32	157	152.10	175	165.63	177	175.50	164	171.10	96	98.59
2067	"	"	36.764	2.172	15 26 08	1.65	160	155.24	175	168.09	181	178.59	168	173.23	102	98.52
2074	"	"	36.497	2.372	15 28 08	0.97	157	154.99	177	167.74	181	178.03	165	172.87	97	97.08
2078	"	"	36.331	4.425	15 29 03	0.33	155	149.35	172	163.15	174	172.20	161	168.85	110	96.00
2059	37.5	8.7	38.365	8.818	15 23 44	0.39	142	134.23	156	151.79	157	158.13	152	159.27	118	117.03
2068	47.6	10.2	41.708	12.046	15 26 14	0.98	98	118.57	134	140.47	140	143.42	137	150.20	102	156.72
2077	37.9	8.2	38.356	8.830	15 28 54	2.59	136	134.22	142	151.77	158	158.10	153	159.25	117	116.98
2094	38.0	6.0	43.689	7.905	15 51 58	1.38	148	120.79	164	147.19	170	152.93	160	157.43	–	145.76
2124	"	"	37.736	5.662	15 59 57	0.73	147	143.58	165	159.44	164	167.93	159	165.90	–	106.09
2108	38.5	9.0	38.737	9.701	15 57 00	0.97	138	131.34	162	149.47	156	155.16	154	157.29	–	123.64
2111	43.5	11.0	39.548	3.609	15 57 39	2.68	113	145.98	143	163.08	139	173.50	144	169.53	–	114.83
2120	38.0	4.0	39.950	3.243	15 59 01	2.09	148	146.28	171	163.74	175	174.60	164	170.20	–	116.48
2137	38.9	7.1	38.397	6.487	16 23 01	0.72	145	140.04	157	157.02	161	164.99	156	163.95	123	111.95
2143	38.1	5.7	37.914	5.874	16 24 15	1.38	145	142.66	169	158.82	162	167.19	160	165.40	–	107.58
2148	43.8	10.3	44.340	8.916	16 25 52	1.73	119	115.84	143	143.40	146	147.43	146	154.43	161	151.52
2157	"	"	39.699	13.567	16 28 23	1.28	121	121.08	144	140.19	139	143.19	145	149.04	176	159.61
2158	"	"	41.139	12.494	16 28 30	0.94	–	119.34	145	140.37	140	143.33	145	149.83	159	157.35
2149	41.1	9.2	38.201	10.257	16 26 01	1.67	133	131.28	155	148.85	150	154.28	150	156.55	133	120.70
2156	"	"	38.216	10.250	16 27 42	1.76	132	131.27	155	148.85	149	154.28	152	156.55	128	120.83
2159	"	"	38.216	10.288	16 28 46	0.63	131	131.18	153	148.77	150	154.17	151	156.48	131	121.00
2166	41.5	7.5	38.249	9.690	16 50 22	1.91	131	132.45	157	150.01	150	155.79	151	157.62	–	118.88
2192	"	"	37.388	8.912	16 56 43	0.91	134	136.03	160	152.51	153	158.88	155	159.64	–	107.81
2171	42.0	11.0	39.589	11.071	16 52 33	1.20	124	126.30	151	145.52	143	150.09	148	153.98	–	138.33
2204	"	"	36.783	-52.986	16 58 31	3.27	123	87.03	151	261.12	142	81.56	149	78.29	–	112.73

FLASH IDENTIFICATION NUMBER	FLASH LOCATION				TIME OF FLASH (GMT)	ATD RESID	BEARINGS FROM EACH CRDF STATION TO A FLASH FIX									
	CRDF FIX		ATD FIX				CAMBORNE		SHANWELL		HEMSBY		LERWICK		MALTA	
	°N	°E	°N	°E	HH MM SS	μS	CRDF	ATD	CRDF	ATD	CRDF	ATD	CRDF	ATD	CRDF	ATD
2173	39.0	11.5	38.347	10.563	16 52 52	1.16	131	130.29	153	148.04	149	153.25	151	155.86	-	123.73
2177	"	"	38.362	10.567	16 54 10	2.12	131	130.25	153	148.02	148	153.22	149	155.84	-	123.91
2174	38.5	5.0	36.800	3.780	16 53 16	0.29	149	150.45	171	164.36	173	173.89	162	170.00	-	98.90
2180	"	"	38.348	4.970	16 54 31	1.37	148	144.34	167	160.61	170	169.68	161	167.08	-	109.45
2182	"	"	40.040	4.408	16 55 02	4.56	142	142.34	170	160.69	169	170.55	161	167.62	-	118.76
2186	"	"	36.665	3.287	16 55 49	2.02	149	152.08	174	165.56	174	175.36	164	171.01	-	98.04
2176	46.5	14.5	45.309	14.530	16 53 44	5.38	89	102.55	131	128.26	117	126.27	136	140.69	-	176.25
2185	38.5	2.5	36.326	2.195	16 55 14	3.20	156	155.74	170	168.21	181	178.55	166	173.26	-	96.17

CRDF stations. Both of these are shown with an ambiguity of 180 degrees appropriate to the CRDF method. The ATD fix for flash 2204 is supported by both CRDF and ATD measurements on activity within 0.5° of this location during this time period. Clearly, in this instance the two systems selected different flashes.

Fig. 4 highlights the significant discrepancies between CRDF and ATD fixes. However, as no bearings were available from the Gibraltar CRDF site and some were missing from Malta, the discrepancies between CRDF and ATD bearings are much more significant than fixing discrepancies in a general interpretation of this data. As Table 1 shows, these bearing discrepancies amount to several degrees. Note that CRDF bearings that are composited to form a single CRDF fix are often scattered over several degrees showing that the internal evidence of these CRDF fixes is weak.

It is evident from Fig. 4 that the independent ATD fixes sometimes form nearly co-located groups of ATD flashes. Of the 41 flashes discussed, no fewer than 17 occur in groups each covering areas of 1.7 - 10.7 km diameter. Table 2 tabulates these in their groups, in order of increasing group diameter, and in chronological order within each group. It is unlikely that such tight geographical grouping occurred by chance within the relatively large region displayed; it is more plausible that several flashes from isolated storm cells or areas of activity have been located. The time proximity of the flashes within the five tightest groups supports this

TABLE 2 – COMPARISON OF CRDF AND ATD FLASH DATA: ATD GROUPING

FLASH IDENTIFICATION NUMBER	ATD FLASH LOCATION °N	°E	TIME OF FLASH (GMT) HH	MM	SS	BEARINGS FROM EACH CRDF STATION TO A FLASH FIX CAMBORNE CRDF	CAMBORNE ATD	SHANWELL CRDF	SHANWELL ATD	HEMSBY CRDF	HEMSBY ATD	LERWICK CRDF	LERWICK ATD	MALTA CRDF	MALTA ATD
2173	38.347	10.563	16	52	52	131	130.29	153	148.04	149	153.25	151	155.86	–	123.73
2177	38.362	10.567	16	54	10	131	130.25	153	148.02	148	153.22	149	155.84	–	123.91
2055	36.518	2.355	15	23	07	156	155.02	176	167.77	181	178.07	166	172.90	98	97.19
2074	36.497	2.372	15	28	08	157	154.99	177	167.74	181	178.03	165	172.87	97	97.08
2149	38.201	10.257	16	26	01	133	131.28	155	148.85	150	154.28	150	156.55	133	120.70
2156	38.216	10.250	16	27	42	132	131.27	155	148.85	149	154.28	152	156.55	128	120.83
2159	38.216	10.288	16	28	46	131	131.18	153	148.77	150	154.17	151	156.48	131	121.00
2053	38.361	8.808	15	22	48	143	134.26	–	151.82	157	158.16	154	159.29	123	116.96
2059	38.365	8.818	15	23	44	142	134.23	156	151.79	157	158.13	152	159.27	118	117.03
2077	38.356	8.830	15	28	54	136	134.22	142	151.77	158	158.10	153	159.25	117	116.98
2082	38.363	8.855	15	29	34	143	134.14	–	151.71	159	158.02	155	159.20	129	117.13
2045	41.646	11.972	15	21	13	118	118.90	144	140.72	141	143.76	146	150.41	163	156.03
2068	41.708	12.046	15	26	14	98	118.57	134	140.47	140	143.42	137	150.20	102	156.72
2075	43.601	7.891	15	28	17	120	121.17	146	147.37	152	153.17	–	157.54	150	145.38
2094	43.689	7.905	15	51	58	148	120.79	164	147.19	170	152.93	160	157.43	–	145.76
2047	38.302	5.077	15	21	27	145	144.12	170	160.39	170	169.37	163	166.88	111	109.27
2180	38.348	4.970	16	54	31	148	144.34	167	160.61	170	169.68	161	167.08	–	109.45

view, although the last two groups extend over a time duration longer than the lifetime of a single convective cell. Thus although we have no independent evidence that the grouped flashes were physically emitted from identical locations, it seems plausible that some flashes are being fixed with a consistency of 2-11 km, well within the accuracy of 40-60 km predicted for this region in Fig. 2 for 25 μs ATD.

Examination of Table 2 for the scatter in ATD "bearings" for flashes within a single ATD group reveals a standard deviation of the order of a few hundredths of a degree for the tightest groups, increasing to a few tenths of a degree for the more doubtful looser groups. This is a substantial improvement over the scatter in CRDF bearings for a composite CRDF fix.

With the hindsight of ATD grouping, it is interesting to observe in Table 2 the scatter of CRDF bearings within ATD groups. Apart from some problem bearings which highlight the CRDF operator's dilemma discussed above, the CRDF bearings for the first five groups are now consistent to within a degree or two, considerably improved over composite CRDF grouping shown in Table 1. Thus internal CRDF evidence supports the ATD grouping to some extent.

Examination of the ATD fixes within each of the first five ATD groups in Table 2 shows an easterly movement with time. The movement is not regular; the same physical point of each

cell is not being tracked, but the drift velocities implied by the time values are not inconsistent with the surface wind velocity implied by the Meteorological Office's archived analyses of this period. Thus the consistency of flash fixing may be even higher than implied by the group diameters.

ATD evidence suggests that member flashes of the individual ATD groups in Table 2 were nearly co-located, implying that the ATD system can produce consistent fixes, although this evidence cannot reveal systematic location errors. By contrast, Fig 4 and Table 1 show that the CRDF fixes corresponding to the member flashes of each ATD group may be scattered over considerable distances. For example the four ATD fixes near 38.36°N 8.82°E have corresponding CRDF fixes separated by up to 808 km, yet the CRDF bearings in Table 2 offer little evidence that the two systems selected different physical flashes. This suggests considerable scatter in the overall CRDF product. Modifying the choice of rejected CRDF bearings would produce different composite CRDF fixes, but it is evident that the need for correct interpretation of CRDF bearing data imposes severe limitations on the reliability of the CRDF product, making it too inaccurate to judge ATD results in detail.

Although there are discrepancies between individual flashes, both CRDF and ATD show activity within the Mediterranean area, with little activity over Europe. It is interesting that the ATD system has a more marked tendency

to locate flashes over the sea, or at least near the coast, than the CRDF system. This might be expected in Winter.

(ii) A Summer comparison. On the basis of the trial evidence, there is less tendency for several flashes to be received from single isolated storm cells, so that it is more difficult to demonstrate consistency in flash fixing. Instead, CRDF/ATD comparisons tend to agree in showing similar areas of diffuse activity, although the actual area of activity may have a better defined structure. Fig. 5 shows all the four-station ATD fixes associated with CRDF fixes that occurred within the displayed region on 13 July 1979 between 1920-2100 hrs GMT. The general agreement is clearly visible, although the ATD system tends to locate flashes over the land area more than the CRDF. This might be expected in Summer.

(iii) Conclusions. It is not appropriate to present further comparisons here to this level of detail. The diagrams presented are not untypical; there is no evident discrepancy between ATD and CRDF fixes, although the ATD fixes appear to be considerably more consistent. The areas in which ATD fixes were obtained were confirmed by the presence of nearby CRDF fixes, and were often confirmed by nearby observer reports.

(d) Ground truth

The high flash-to-flash location consistency of ATD fixes described above is encouraging, but does not provide direct evidence of location accuracy. Systematic errors might allow tight clustering of nearly co-located flashes, but position them in some systematically wrong location. Ideally one might hope to demonstrate coincidences between "known" lightning flash locations and ATD fixes.

In practice, the problem of establishing ground truth in this way has defeated the users of the CRDF system over the 40 years of its operational lifetime. The problem is one of scale and data capture probability. Any practical observer network can only observe flashes over a small fraction of the land area, with relatively poor accuracy, and current reporting methods do not usually time the observed flashes precisely. Conversely, both CRDF and experimental ATD systems cannot hope to detect every lightning flash within an observed area. The requirement for 4-Sferic flashes reduces the proportion of fixed flashes even further. Thus it is difficult to establish coincidence between the observer network and ATD system, and to distinguish these from chance association of poorly-fixed unrelated flashes.

Some weak confirmation can be obtained by noting that ATD fixes do appear to occur in the general areas where synoptic observers report past or present thundery activity, or where

this activity is highly likely from the normal meteorological indicators. Conversely, ATD fixes do not appear to occur in regions where thundery activity would be unlikely in the face of concurrent or subsequent observations interpreted through normal analysis techniques.

On one particular occasion at 1100 hrs on 12 July 1979, several co-located ATD fixes occurred, fairly isolated from other fixes, in an area of 5 km by 2 km at 45°3'N 3°1'E just 20 km to the east of the Plomb du Cantal in the Massif Centrale region of France. There was substantial meteorological evidence to support the existence of intense thunderstorms in this area. The evidence included thunderstorms observed in the general area before and after 1100 hours, evidence of instability in nearby radiosonde ascents, the inference through chart analysis of a small developing thundery low centered near this area, and observed confluent air flow and probably convergence in a topography which might well have funnelled air into the area. Unfortunately, although the meteorological evidence supports the ATD fixes strongly, it cannot be used to position the likely flash locations to better than about 20 km. Thus it is only possible to confirm ATD positioning to this accuracy, although evidence in the following sections suggests that the likely ATD accuracy is much higher than this. This appears to be the accuracy limit of "ground truth" observations.

(e) RESIDUAL as a measure of flash location accuracy

Appendix D describes the flash fixing process in terms of the minimisation of the dimensionless quantity RESIDUAL. For maximum fix accuracy, the differences between theoretical and measured ATD values are weighted by the reciprocal of the estimated standard deviation $\sigma(r)$ of the difference for each r. For trial analysis the values of σ were assumed equal for all r, but unknown: one trial objective was to determine σ under experimental conditions so that expected accuracy charts could be constructed for any proposed network geometry. Thus, the values of σ in Appendix D's expression for RESIDUAL were replaced by a non-dimensional value of unity, giving a modified RESIDUAL having the dimensions of time. The value of the modified RESIDUAL might be expected to be root mean square σ as the expression is correctly normalised for the available degrees of freedom.

The contour map of Fig. 2 was calculated using the Monte-Carlo method described above; and for the same trial geometry and 25 μs ATD perturbations an attempt was made to plot a contour map of calculated modified RESIDUAL. This was abandoned after considerable computer resources had been expended when it became clear that no significant geographical structure existed: the chart was uniform at 25.0 μs within the noise levels of around $\pm$0.5 μs implied by the limited numbers of fixes averaged at each grid point. A similar uniform result of 25.0 μs was found for the

seven-station network of Fig. 3. The result appears to hold for all charts provided that the distance between Outstations is substantially greater than the distance travelled by light in σ, in this case 7.5 km.

Fig. 6 shows calculated (Monte-Carlo) histograms of RESIDUAL summed between a geometric progression of values. The two histograms shown are for grid points over the entire chart for the trial network ((a), solid lines) and the seven-station network of Fig. 3 ((b), dashed lines). The root mean square RESIDUAL, sample standard deviation of RESIDUAL, and number of RESIDUAL values used were (25.08 μs, 15.03 μs, 25189) and (24.95 μs, 8.43 μs, 25560) for the trial and seven-statiion networks respectively. Neither of the RMS values of RESIDUAL is significantly different from 25.00 μs given the respective sample standard deviation and sample population.

For the trial network, two regions of 7° east by 14° north were centred over areas of high and low flash location accuracy respectively. The sample standard deviations were calculated at 15.03 μs and 15.07 μs respectively, indicating that the standard deviation as well as the RMS RESIDUAL appears to be constant with chart position.

Thus we have a quantity RESIDUAL whose RMS value and distribution appears to be independent of flash location, so that all experimental flashes can contribute to the estimation of its statistical moments. As the value of

RESIDUAL approximates σ, a knowledge of the experimental RMS RESIDUAL for one network allows the accuracy of that network, or any other network, to be predicted.

The invariance of the RESIDUAL distribution means that the value of RESIDUAL for a single flash can be compared with the limits of the theoretical or measured distribution, and an outlying value warns of possible problems. For the trial network the broad distribution limits the quality assurance available, but a seven-station network appears more promising. The reason for the latter's smaller standard deviation is because RESIDUAL is a form of RMS measure of the ATD differences, averaged over the available degrees of freedom (m-2). These number one for a four-station network, and four for a seven-station network, explaining the ratio of approximately two in standard deviation. In practice, any deviation from the shape of a Chi-square distribution, which should give an accurate 2:1 ratio, is probably due to deficiencies in the random-number generator used.

The use of RESIDUAL for quality control and predicting chart accuracy assumes that the values of σ for the various ATD differences are equal, and that for a theoretical flash location coincident with the actual flash location the expectation values for the ATD differences are each zero. For experimental data using the flash fixing techniques of Appendix D this will not be the case because of the systematic errors introduced by propagation effects. Where the systematic effects may be large compared with random

effects (eg noise, encoding problems etc.) the comparisons with a Gaussian model must be interpreted with care. Some quantification of this can be achieved by examining recorded waveforms, or the effects of a propagation model, and comparing the ATD obtained by correlogram or main peak matching with that obtained by attempting to match the dispersion-free ground-wave in the early portion of the Sferic. Discrepancies of around 10 μs or less are apparent in most waveform pairs, so that comparison with a 25 μs standard is probably reasonable. Any technique which can alleviate the systematic propagation effects will make the comparison with a Gaussian model more realistic.

(f) RESIDUAL as a measure of trials data accuracy

As described above, histograms and statistical moments of RESIDUAL provide a powerful tool for determining the ATD accuracy of trial data. Thus all four-Sferic flashes were fixed using the methods of Appendix D, and histograms constructed for all flashes which were within an area of 0°N to 80°N, and 80°W to 80°E.

Initial histograms were disappointing, producing shapes having little resemblance to Fig. 6(a). However, the

time-ordered data included long sequences of low values of RESIDUAL interspersed with long sequences of substantially higher values with no obvious differences in the flash populations. Close scrutiny of the sequences having the largest RESIDUAL revealed ATD values that exceeded the physical maximum: the light travel-time between Outstations. It was clear that in spite of all the effort spent on aligning timescales (a necessary support activity not emphasised in this paper) the frequent problems of Outstation clock-jumps combined with the many ambiguities of the epoch calibration methods used had produced "corrected" timescales containing large errors. At a later date, methods of resolving systematic timescale errors were developed which demonstrated the reality of timescale errors in this data. However, at this time a crude approach was taken to remove the worst of the corrupted data without attempting to correct it: any long sequences of Sferics with most values of RESIDUAL greater that 50 μs, or greater than three times the RMS RESIDUAL of the remaining data, were ignored. This method provides no guarantee of eliminating all significant timescale errors, and evidence of some remaining problems is discussed below, but it was the only feasible method with the limited resources available.

Table 3 lists the results of this selection process for the four usable trial periods labelled in Column 1. Column 2 lists the number of four-station flashes falling within the geographical area and contained within acceptable sequences of data. Column 3 shows the number of contiguous sequences

of acceptable flashes extracted from each trial period, while Column 4 indicates the proportion of acceptable four-station flashes from those that merely fell within the geographical area. The most careful work on timescale alignment was done on trial (a), and as a result nearly 90% of the data is acceptable with just two short "bad" patches being rejected. More typically, one or two sequences of usable data was recovered from each trial, covering around 50-60% of the available data. Although it was clear that further work should increase the recovery rate and improve the data quality, it was felt that these results vindicated the technique without incurring further effort.

TABLE 3 - STATISTICS OF ACCEPTABLE FLASH SEQUENCES

Trial Period	No of Flashes Accepted	No of Contiguous Sequences	% of Available Flashes	RESIDUAL (RMS μs)
22.11.78- 6.12.78 (a)	1085	3	87	3.3
5. 6.79-15. 6.79 (b)	316	2	48	10.9
10. 7.79-20. 7.79 (c)	394	2	60	5.1
4. 9.79-14. 9.79 (d)	455	1	57	5.2

Histograms of cumulated acceptable sequences for the four Trial Periods of Table 3 are shown in Fig. 7. Trial Period

(a) has a shape similar to the theoretical curve of Fig. 6 (a), while peaking at a low value of RESIDUAL below 4 μs, and reducing sharply to the right. Trial Periods (c), (d) and especially (b) are less well shaped, probably because of small timescale errors as other indications such as signal-to-noise ratio are comparable for all Trial Periods. All the histograms show small peaks near RESIDUAL values of 100-160 μs, probably associated with mis-matching waveforms by a single cycle. Other peaks at higher values are probably associated with completely spurious matches.

All the Trial Period histograms, with the possible exception of (b), exhibit a population gap near a RESIDUAL of 40 μs. Thus 40 μs appears to be a suitable upper limit for acceptable flashes which will reject "rogues" efficiently. The RMS RESIDUAL values listed in Table 3 are calculated for each Trial Period from flashes with RESIDUAL below 40 μs. It can be seen that all this data exhibits values of RMS RESIDUAL well below the target of 25 μs, and the most trustworthly Trial Period (a) value is 3.3 μs. Thus, provided that the technical problem of maintaining accurate timescales can be overcome, and flashes with a RESIDUAL greater than 40 μs are rejected, an ATD system should be well able to exceed the calculated accuracy shown in Fig. 3 for a 25 μs RMS RESIDUAL.

This method of investigating the accuracy of the ATD principle has the advantage that there is no need for CRDF data for comparison, and that the results of over two

thousand four-Sferic flashes can be displayed conveniently.

The ATD/CRDF comparison was not able to show up systematic errors in the ATD fixes. Although this method cannot guarantee to eliminate the effects of systematic errors (the effects of propagation have only been removed to zero-order, see Appendix D) it is difficult to conceive of substantial systematic errors that will not increase RESIDUAL. Thus it appears likely that any systematic errors in flash positioning are below the limits shown for the 25 μs error-maps.

6. CONCLUSIONS

A new technique (Arrival Time Difference, or ATD) for the remote location of lightning flashes to ranges of several thousand kilometers is described, and compared with the present operational Cathode Ray Direction Finding (CRDF) system. The new technique does not suffer from many of the operational limitations of the CRDF system, and has the potential for substantially improved accuracy if an ATD accuracy of 25 μs can be achieved. Fig. 3 illustrates a calculated flash location accuracy chart for an assumed 25 μs ATD accuracy. However, the ATD technique suffers from lightning waveform propagation effects whose practical impact needs to be quantified.

The techniques and results of a series of careful measurement trials are presented and analysed in various ways. Direct comparison between ATD and CRDF methods is difficult for a number of operational reasons. However, such comparison indicates that flash fixing accuracy with the ATD technique is an order of magnitude or so more consistent than that for the CRDF technique, and does not appear to demonstrate any systematic bias. An attempt was made to compare the ATD flash location results with meteorological "ground truth", but the accuracy of comparison with available data appears to be considerably less than the accuracy of ATD flash location.

An alternative analysis technique is presented which examines a measure of the internal inconsistency of ATD flash fixes (the "RESIDUAL") and is based solely on ATD evidence. This technique reveals that great care must be taken in analysis to make best use of the experimental data quality. However, if this is done, the technique demonstrates from the experimentally measured data that the ATD accuracy can be improved by a factor of one half to one orders of magnitude above the 25 μs standard, giving a correspondingly improved chart accuracy over Fig. 3.

The RESIDUAL technique highlights the difficulty of establishing adequate timescales at ATD Outstations, but provides a method for determining when this has been achieved.

ACKNOWLEDGEMENTS

The author is indebted to the staff of the Meteorological Office who contributed to the trials, especially those who gave long and irregular hours to gathering the data; and to the officers at RAF North Front (Gibralter) for allowing their Mess to be used as a laboratory to reduce the effects of the Spanish transmitter. My thanks are also due to the staff at the Time Division of the National Physical Laboratory for the loan of a travelling atomic clock, and for their cheerful acceptance of its demise.

REFERENCES

Adcock, F. and Clarke, C. 1947 The location of thunderstorms by radio direction-finding, London, J. Inst. Elect. Eng., 94, 118-125.

Alpert, J.L., Fligel, D.S., and Michailova, G.A. 1967 The propagation of atmospherics in the earth-ionosphere waveguide, London, J. Atm. Terr. Phys., 29, 29-42.

Arnold, H.R. and Pierce, E.T. 1964 Leader and junction processes in the lightning discharge as a source of

VLF atmospherics, Washington, Nat. Bur. Stand., Rad. Sci. J. Res., 68D, 771-776.

Bomford, G. 1980 Geodesy, Clarendon Press, Oxford

Budden, K.G. 1951 The propagation of a radio-atmospheric, London, Phil. Mag., Ser 7, Vol. 42, 1-19.

Challinor, R.A. 1967 The phase velocity and attenuation of audio-frequency electro-magnetic waves from simultaneous observations of atmospherics at two spaced stations, London, J. Atm. Terr. Phys., 29, 803-810.

Chapman, F.W., Llanwyn-Jones, D., Todd, J.D.W., and Challinor, R.A. 1966 Observations on the propagation constant of the earth-ionosphere waveguide in the frequency band 8 c/s to 16 c/s., Washington, Nat. Bur. Stand., Rad. Sci. J. 1, 1273-1282.

Horner, F. 1953 Radio direction finding: influence of buried conductors on bearings, Wireless Engineer, 30, 187-191.

Horner, F. 1954(a) New design of radio direction finder

for locating thunderstorms, London, Meteor. Mag., 83, 137-138.

Horner, F. 1954(b) The accuracy of the location of sources of atmospherics by radio direction-finding, London, Proc. Inst. Elec. Eng., Part III, 101, 383-390.

Horner, F. 1964 Radio noise from thunderstorms, Saxton, J.A., Adv. Radio. Res., 2, 121-204, Acedemic Press.

Keen, R. 1938 Wireless direction finding, Iliffe and Sons Ltd., Dorset House, Stamford St. London SE1. (Chapel River Press, Andover, Hants.).

Lewis, E.A., Harvey, R.B., and Rasmussen, J.E. 1960 Hyperbolic direction finding with sferics of transatlantic origin, J. Geophys. Res., 65, 1879-1905.

Maidens, A.L. 1953 Methods of synchronising the observations of a 'sferics' network, London, Meteor. Mag., 82, 267-270.

Meteorological Office 1975 Annual Report on the Meteorological Office 1974, 34-35. London HMSO. Met. O. 881, ISBN 0 11 400288 6.

Norinder, H. 1954 The wave-forms of the electric field in atmospherics recorded simultaneously by two distant stations, Stockholm, Ark. Geof., 2, 161-195.

Ockenden, C.V. 1947 Sferics, London, Meteor. Mag., 76, 78-84.

Peterson, W.W. and Weldon, E.J. 1972 Error-correcting codes, second edition, MIT Press.

Schonland, B.F.J., Elder, J.S., Hodges, D.B., Phillips, W.E., and van Wyk, J.W. 1940 The wave-form of atmospherics at night, London, Proc. R. Soc., 176A, 180-202.

Schwartz, M. 1970 Information transmission, modulation, and noise, McGraw-Hill Inc.

Shannon, C.E. 1949 Communication in the presence of noise, Proc. Inst. Radio Engineers, 37, 10-21.

Wait, J.R. 1961 A diffraction theory for LF sky-wave propagation, J. Geoph. Res., 66, 1713-1724.

Wait, J.R. and Walters, L.C. 1963 Reflection of VLF radio waves from

an inhomogeneous ionosphere. Part I, exponentially varying isotropic model, Washington, Nat. Bur. Stand., J. Res., 67D, 361-367.

Watt, A.D. 1967 VLF Radio Engineering, International Series in Electromagentic Waves, Volume 14, Pergamon Press.

Yamashita, M. and Sao, K. 1974(a) Some considerations of the polarisation error in direction-finding of atmospherics II. Effect of the inclined electric dipole, London, J. Atm. Terr. Phys., 36, 1633-1641.

Yamashita, M. and Sao, K. 1974(b) Some considerations of the polarisation error in direction-finding of atmospherics I. Effect of the earth's magnetic field, London, J. Atm. Terr. Phys., 36, 1623-1632.

APPENDIX A

THE SFERICS FILTER PROFILE

(a) Introduction

The basic concepts and design of the analogue filters used in the Sferics Filter have a profound influence on the success of the analysis methods, and so brief details are presented here.

(b) The broad-band filter

The spectral profile of this filter dominates the system's time-domain response to any impulsive or Sferic-like waveform. It contains a high-pass 5-pole Butterworth filter exhibiting a 3 dB pass-band limit at 2.0 kHz, intended to remove large amplitude low-frequency noise, and any mains-related interference. The high-pass filter is cascaded with a 0.1 dB ripple low-pass 6-pole Chebychev filter having a 0.1 dB band-pass limit at a nominal

22.88 kHz. This low-pass filter exhibits 51.6 dB attenuation at 50 kHz, the Nyquist frequency for the sampling rate used.

The broad-band filter combination exhibits a Group Delay varying between 40-85 μs within the Sferic spectral peak region of 7.5-27 kHz. Although the Group Delay becomes larger at lower frequencies, peaking at 460 μs near 2 kHz, the earth-ionosphere waveguide attenuation maximum of around 30 dB per Mm at 2 kHz (Challinor, 1967) ensures that this effect is not obtrusive with Sferic waveforms, which thus suffer little distortion. The filter impulse response has dropped to negligible levels (for an 8-bit quantiser) by 1 ms after a test impulse, ensuring that a Sferic waveform is adequately represented by a 10 ms data window.

(c) Notch filters

The Sferics Filter contains four digitally adjustable Notch filters. Each notch filter has a nominal transfer function $T_n(s)$ of the arithmetically symmetrical form:

$$T_n(s) = H(s + j\omega_c) \times H(s - j\omega_c)$$

where s is the complex frequency, j is the square-root of -1, and ω_c is the notch filter centre frequency in radians/sec. H(s) is a high-pass 5-Pole 0.1 dB Chebychev filter which gives $T_n(s)$ at least 33.0 dB attenuation within 50 Hz from the notch centre (a 100 Hz stop-band), 3.0 dB attenuation at 85 Hz either side of the notch centre, and no more than 0.1 dB attenuation outside 96.45 Hz from the notch centre. The centre frequency is phase-locked to the time-keeping oscillator at a frequency of n x $10^7/(2^{20})$Hz (~ n x 9.537 Hz) where n can have integer values.

Notch filters are designed to remove man-made transmissions, and are each just wide enough for this task. A shift in filter profile of 10 Hz would significantly compromise the elimination of interference. However, the filter design is such that changes from nominal characteristic of more than 2 Hz are unlikely.

Notch filters will inevitably distort Sferic waveforms as well as eliminate man-made transmissions. By contrast with the broad-band filter, whose slowly-varying spectral profile implies small group-delay, the abrupt notch filter profile can (with certain tone-burst signals) exhibit "ringing" effects lasting for tens of milliseconds. However, the notch filters are so narrow that these effects are confined to narrow spectral regions with the largest group delays corresponding to heavy attenuation. Thus a Sferic signal, having short duration and a correspondingly wide spectrum,

has only a small fraction of its energy affected by attenuation or large group delays. Thus, although the filter response does include ringing effects whose duration may exceed the data window, they are of negligible amplitude, especially when the filter response is to be used in a correlation process where the square of the amplitude is significant. Notch filters do exhibit small phase shift effects occurring over a wider spectral region, but these are sufficiently slowly-varying to be corrected accurately by spectral correction techniques based on the information in the data window.

Notch filters thus have a small effect of Sferic waveforms. The fact that the notch filter design is highly stable implies that non-catastrophic errors in notch filter profile will have an exceedingly small effect on waveform shape. Thus the effects of the notch filters are highly predictable.

APPENDIX B

SPECTRAL CALIBRATION AND CORRECTION OF THE SFERICS FILTER PROFILE

(a)Measurement of the broad-band filter profile

The Test Signal consists of an m-sequence (Peterson and Weldon, 1972) pseudo-noise generator which goes through 1023 states, each lasting for 10 μs, before repeating. This generates 511 frequencies below the 50 kHz Nyquist frequency for 10 μs sampling, each being a multiple of the fundamental frequency whose period is 10230 μs (~ 97.8 Hz), having nearly equal known amplitudes.

The repetitive Test Signal is applied to the Sferics Filter, including any notch filters, and allowed to run long enough for transient responses to settle. The Sferics Filter response is therefore the sum of the responses to the individual sine-waves, and contains negligible energy above 50 kHz because of the Sferics Filter characteristics.

The analogue response is sampled every 10 μs, and stored as a 1024-point waveform in the Transient Recorder. The first 1023 points are regarded as representative of the repetitive analogue signal, and are transformed to frequency space by 1023-point Discrete Fourier Transform, which analyses the Fourier Series.

The spectrum of the Sferics Filter response is divided by the known 1023-point Discrete Fourier Transform of the Test Signal, and the resulting quotient spectrum is further divided by the "known" 1023-point spectrum of each notch filter present in the Sferics Filter. This leaves the spectrum of the broad-band filter, with some small contamination by profile errors in the notch filters.

(b) Shifting the profile measurements to convenient frequencies

The spectrum of the broad-band filter contains only the discrete frequencies used in the original measurement. However, the broad-band filter's impulse response has a significant amplitude duration considerably less than the 10230 μs data window obtained by performing a 1023-point Inverse Discrete Fourier Transform on the measured broad-band filter spectrum. Thus the time-domain waveform so obtained represents an accurate impulse response of the broad-band filter and is not contaminated by overlapping impulse responses from adjacent repetitive time-windows. This would not have been the case had the notch filters been left in. Thus the 1023-point time-domain impulse-response falls to zero amplitude before the end of the data window, and can be extended to any duration merely by adding samples of zero amplitude. This allows any frequency response to be

calculated through a further n-point Discrete Fourier Transform. The most useful extension is to 1024 samples, which is amenable to computationally efficient Fast Fourier Transform manipulation, giving a Calibration Spectrum based on multiples of the frequency whose period is 10240 μs (~ 97.7 Hz).

(c) Spectral correction

Once the Calibration Spectrum has been obtained, it is used to correct Sferic Waveforms for minor discrepancies in the broad-band filter, and any residual group-delay discrepancies in the notch filters. This is achieved by taking the 1024-point Sferic waveform and transforming to frequency domain. The Sferic spectrum is divided by the measured Sferic Filter spectrum, and multiplied by the theoretical Sferic Filter Spectrum; the result is multiplied by a fixed conditioning spectrum having some attenuation near the broad-band filter pass-band limits to avoid "corrections" which merely amplify noise. Finally, the conditioned spectrum is multiplied by any theoretical notch filter profiles which may be necessary to bring the effective system transfer function to a common mathematical ideal. The result is the spectrum of the Sferic that would have been received through a mathematically ideal Filter. In this frequency domain form it is ready for the extraction of

Time-Difference by the Correlogram technique.

The choice of "conditioning spectrum" is somewhat arbitrary, and with noise-free waveforms of identical shape would not affect the ATD result. However, improved results in the presence of noise are obtained if the overall profile matches the Sferic amplitude envelope to some extent. Thus the conditioning filter was chosen to make the "mathematical ideal" filter a 6-Pole Bessel filter, transformed to a band-pass having geometrical symmetry, with 9.766 kHz centre frequency and 3 dB bandwidth of 5.0 kHz; together with the necessary notch filters.

APPENDIX C

THE EXTRACTION OF "INTER-BOX" ARRIVAL TIME DIFFERENCE BY THE CORRELOGRAM TECHNIQUE

(a) Introduction

Using the Sferics Trial hardware, the ATD between two Sferics received at different Outstations is the sum of two terms:

(i) The time-difference between the first ordinates of the two sampled Sferic waveforms, a calculation involving the conversion of local timescales to International Atomic Time.

(ii) The "Inter-Box Time-Difference". The two data-windows may be envisaged as boxes drawn round the continuous Sferic waveforms represented by the sampled data points. If the Sferic waveforms are now aligned in some "best fit" sense, the Inter-Box Time-Difference is the corresponding time-shift between the boxes.

This Appendix is concerned with the second term only.

(b) Extraction of time-difference

Consider two sampled waveforms $w_0'(t)$ and $w_1'(t)$, where t is time in seconds starting at zero for the first ordinate, each having n samples spaced T seconds apart and thus of finite duration $\tau = nT$. Each is assumed to contain a disturbance of interest surrounded by a region of noise only. Each may be regarded as being sampled from a continuous repetitive waveform, having a repetition period τ, which is uniquely defined by assuming that no energy exists in the continuous waveform above the Nyquist frequency for the sampling rate (Shannon, 1949). Call these repetitive continuous waveforms $w_0(t)$ and $w_1(t)$ respectively.

Regard $w_0(t)$ as a "reference" or "signal"; and $w_1(t)$ as consisting of $w_0(t)$ multiplied by a positive "best fit" amplitude constant α, shifted forward in time by δ, and to have "noise" $n_1(t)$ added:

$$w_1(t) = \alpha w_0(t - \delta) + n_1(t)$$

We can calculate the mean square "noise" $\overline{n_1^2}$ within $w_1(t)$:

$$\overline{n_1^2} = (1/\tau)\int_\tau (n_1(t))^2.dt$$

$$= (1/\tau)\int_\tau (w_1(t))^2.dt - ((2\alpha)/\tau)\int_\tau w_1(t).w_o(t-\delta).dt$$

$$+((\alpha^2)/\tau)\int_\tau (w_o(t-\delta))^2.dt$$

The first term is the mean square of $w_1(t)$, the constant $\overline{w_1^2}$. Similarly, as $w_o(t)$ is repetitive, the third term is α^2 multiplied by the constant $\overline{w_o^2}$. Both of these constants may be calculated from the sampled data. The second term is (-2α) multiplied by the value of the time-lag correlogram CORR(δ) for any value of δ. Eliminate α by minimising n_1 with respect to α :

$$\frac{d\overline{n_1^2}}{d\alpha} = 0 = -2\ CORR(\delta) + 2\alpha\overline{w_o^2}$$

This gives α; and because only positive values of α are meaningful, implies that we must consider only positive values of CORR(δ).

The mean square "signal-to-noise ratio" $R(\delta)$ is given by:

$$R(\delta) = (\alpha^2.\overline{w_o^2})/(\overline{n_1^2}) = \frac{CORR^2(\delta)}{\overline{w_o^2}.\overline{w_1^2} - CORR^2(\delta)}$$

This is maximised, making the waveforms match best, when $CORR(\delta)$ is maximum, giving the intuitively obvious result that the "best fit" time-difference of $w_1(t)$ with respect to $w_o(t)$ is the value of δ which gives the highest positive peak in the continuous (repetitive) correlogram $CORR(\delta)$. Note that for identically shaped repetitive waveforms the maximum $R(\delta)$ is infinite.

(c) Use of $R(\delta)$

For typical Sferic waveforms $CORR(\delta)$ exhibits several positive peaks during correlation of the actual disturbances. The highest is likely to match corresponding portions of the physical waveforms, but propagation distortion and additive interference may emphasise an incorrect peak to maximum. The relative heights of peaks in $CORR(\delta)$ provide little warning of this as a pair of "wave-packet" disturbances may produce many nearly equal peaks even when a visual waveform comparison gives no doubt of the correct match. The function $R(\delta)$, expressed in dB, provides improved discrimination: a large main peak R implies nearly identical

waveforms with low probability of mismatch.

Another useful discriminant is the "relative signal-to-noise ratio". This is $R(\delta)$ in dB for the second highest positive peak minus $R(\delta)$ in dB for the highest positive peak. A small value warns of uncertainty between two peaks.

Correctly filtered Sferics of interest often dwarf background noise, so similar propagation paths imply large R. A second unwanted Sferic within the data window, even if overlapping the first, reduces peak R, warning of the potential for catastrophic degradation of the measured ATD.

(d) Digital extraction of δ, $R(\delta)$

The mathematical form for correlation between two waveforms is identical to the convolution of the first waveform with the time-reversed second waveform. This leads to the well-known result that the correlogram can be obtained by taking the Fourier Transforms $W_1(s)$, $W_o(s)$ of $w_1(t)$, $w_o(t)$ respectively, multiplying $W_1(s)$ by $W_o^*(s)$ where asterisk represents a complex conjugate, and then taking the inverse Fourier Transform. The relevant peaks may now be found by

inspection.

The above is a continuous waveform description. With sampled waveforms the process is identical, but "dashed" (sampled) waveforms and spectra, and the Discrete Fourier Transform are used. Unfortunately, the result is a sampled correlogram, with no guarantee that the required peak lies on a sample point. The digital process is thus modified slightly to shift the peak iteratively onto a sample point, as these are true values of the underlying continuous repetitive waveform.

Using the complex conjugate form of the Discrete Fourier Transform, we obtain (Appendix B) the spectrum of the reference waveform, take the complex conjugate by changing the sign of the imaginary elements, and multiply element by element by $(1 - y\omega)$ where ω is the element angular frequency, and y is a scaling factor discussed below. The result is multiplied by the spectrum of the second waveform, and the inverse Discrete Fourier Transform taken. The original waveforms were wholly real, so that the correlogram is real, and in the real field of the result. The imaginary field contains the time derivative of the correlogram (as $-\omega$ is js) multiplied by the scaling factor y, whose value is chosen to roughly equalise the numerical values in the time-domain real and imaginary fields to avoid degradation of the correlogram

or its derivative through numerical truncation. Thus:

$$\mathrm{CORR}(t) + jy \frac{d}{dt} \mathrm{CORR}(t) = L^{-1} \left\{ W_1'(s) \; (1-y\omega) \; W_o'^{*}(s) \right\}$$

The sampled values of CORR(t) are examined to identify the pair of large positive amplitude successive samples, whose derivative is positive followed by negative, most likely to straddle the highest peak. The position of the peak is now "roughly" estimated by linear interpolation to find t for zero derivative. This makes the effective assumption that the peak is parabolic between the two straddling sample points. The time Δt by which the correlogram has to be delayed to shift this estimate onto the nearest sample point is calculated.

The process is now iterated by taking the spectrum of the correlogram and its scaled derivative, multiplying by $\exp(-s\Delta t)$ to shift the estimated peak to a sample point, and taking the inverse Discrete Fourier Transform to produce the shifted composite correlogram and derivative. This is iterated as required. After the final iteration, the peak position is found by linear interpolation of the derivative, and the peak value is found by fitting a parabola to the sample point nearest the peak and those two adjacent.

For the Sferics Trial 1024-point Discrete Fourier

Transforms were used throughout. These produce "theoretically correct" results, and by the second linear interpolation produce an ATD which generally differs from iteration-to-convergence by less than 0.1 μs. However, the iterative process can be performed on a "windowed" limited time region, centered on the estimated peak, to reduce computation at the expense of an insignificant error in ATD. The algorithm described above may be made computionally fast, but does suffer from the weakness that the highest peak must be identified from the sampled data points of the first iteration. In practice, provided that a "mathematical ideal" filter of adequate bandwidth is chosen (Appendix B), the natural waveshape provides a signature which makes the highest peak sufficiently obvious on most occasions, as evidenced by the histograms of Fig. 7.

APPENDIX D

FLASH FIXING

The process of Flash Fixing is described here in a generalised form suitable for any number of Outstations, although the Sferics Trial comprised only four.

Sferic waveform data are sorted into roughly chronological

order (by the epoch of the first ordinate of the waveform) and grouped into "Flashes". The time boundaries between Flashes are established by the requirement that ATD values must not exceed the theoretical maximum: the transit time for a radio-wave to travel between a pair of Outstations. Flashes comprising fewer than four Sferics are discarded.

In order to select the "Reference" Outstation, the Outstations included in a Flash are ranked on the basis of their geographical position and the known accuracy of conversion between their local timescales and a common timescale such as International Atomic Time (IAT). An Outstation near the network centre is more likely to minimise differential propagation effects, but the actual choice is intended to minimise overall ATD errors to produce the most accurate fix. The Sferics in a Flash are spectrally corrected (Appendix B) and the ATD between the Reference Outstation Sferic and each of the others is determined (Appendix C).

The first stage of Flash Location is to find an approximate fix using an analytical method based on three carefully selected ATD values and a spherical earth model which assumes velocity-of-light Sferic propagation. This non-iterative method does not give the most precise result, especially in the face of ATD errors, but suffices as a starting estimate for the main iterative algorithm, thus reducing eventual processing load.

The main Flash Fixing algorithm is an iterative process that minimises the function RESIDUAL (ϕ,λ), where:

$$\text{RESIDUAL}^2(\phi,\lambda) = (1/(m-2)) \sum_{r=1}^{m} \left(\frac{ATD_{TH}(r,\phi,\lambda) - ATD_M(r)}{\sigma(r)} \right)^2$$

RESIDUAL is a function of the estimated flash position in terms of its geodetic latitude (ϕ) and longitude (λ). This is calculated using the m values of measured ATD (ATD_M) and the m "theoretical" ATD values (ATD_{TH}) calculated in turn from the known Outstation geodetic co-ordinates, and the geodetic co-ordinates (ϕ,λ) of the fix estimate. The difference between these ATD values for the true fix is assumed to have a Gaussian distribution of zero mean and variance σ^2. Thus the squared ATD differences are correctly weighted for combination into an overall root-mean-square value, and a normalising factor (m-2) is used to account for the two degrees of freedom lost in calculating ϕ,λ. As the expectation value for the square ATD differences is σ^2, the expectation value for RESIDUAL after minimising with respect to ϕ,λ is unity; the minimum occurring at the most likely fix. The distribution of RESIDUAL^2 is normalised Chi-square, although it is convenient to plot it in the form of Figs. 6 and 7.

The fix co-ordinates are systematically adjusted using a second-order algorithm for minimising RESIDUAL until a

suitable convergence level is reached.

The value of ATD_{TH} is based on velocity-of-light propagation along the geodesic (shortest surface distance) between (ϕ,λ) and the relevant Outstation, assuming a spheroidal earth with equatorial radius of 6378200m and a flattening factor of 1/298.3. The geodesic was calculated using Rudoe's reverse formula (Bomford, 1980).

The values to be attributed to σ^2 can be calculated as the sum of a number of terms. The error in local timescale conversion to IAT can be estimated from a knowledge of the methods used for maintaining the conversion. Noise and propagation effects can be crudely estimated using signal-to-noise ratio, relative signal-to-noise ratio (Appendix C), and the approximate flash location together with a knowledge of likely propagation effects. Such techniques give the algorithm a degree of robustness against failed equipment or "bad" data such as overlapping or noisy Sferics. For the Sferics Trial results, however, this level of sophistication was not used: the values of σ^2 were set equal, giving a less than optimum fix.

The "velocity of light" must be quantified as wave-guide velocities differ from free-space velocities. A phase velocity is appropriate as the Correlogram ATD attempts to match corresponding waveform phases, and in a wave-guide this can exceed free-space velocity.

A pragmatic fit of various velocities to Trial measurements was attempted, including both day and night results, and a multiplier on unbounded vacuo light velocity of around 1.004 was found to reduce the RMS value of RESIDUAL below that for a 1.000 multiplier by a factor between 2 and 4. The intermediate results obtained in determining this multiplier were examined critically to disprove any significant effects by small systematic experimental errors.

For theoretical support of the optimum multiplier, a wave-hop model (Watt,1967) was used to propagate a radiation source function consisting of the differential of a Dirac Impulse (after Budden, 1951) to various ranges, filtering the result through the "mathematical ideal" filter of Appendix B. An ATD was extracted between pairs of these filtered waveforms, and interpreted as a velocity over the differential range. The velocity obtained varied with the conditions assumed, but for differential ranges of 150-650 km and average ranges of 1000-3000 km (covering the bulk of a useful Service Area) multipliers between 1.001 and 1.007 were calculated, with a value of 1.004 appearing as a reasonable general fit.

On the basis of the above evidence a multiplier of 1.004 was chosen, giving a "velocity of light" appropriate to the "mathematical ideal" filter of Appendix B of 300991 metres/sec. This was used to provide a "zero-order correction" for propagation effects in the analysis of all the trial data for this paper.

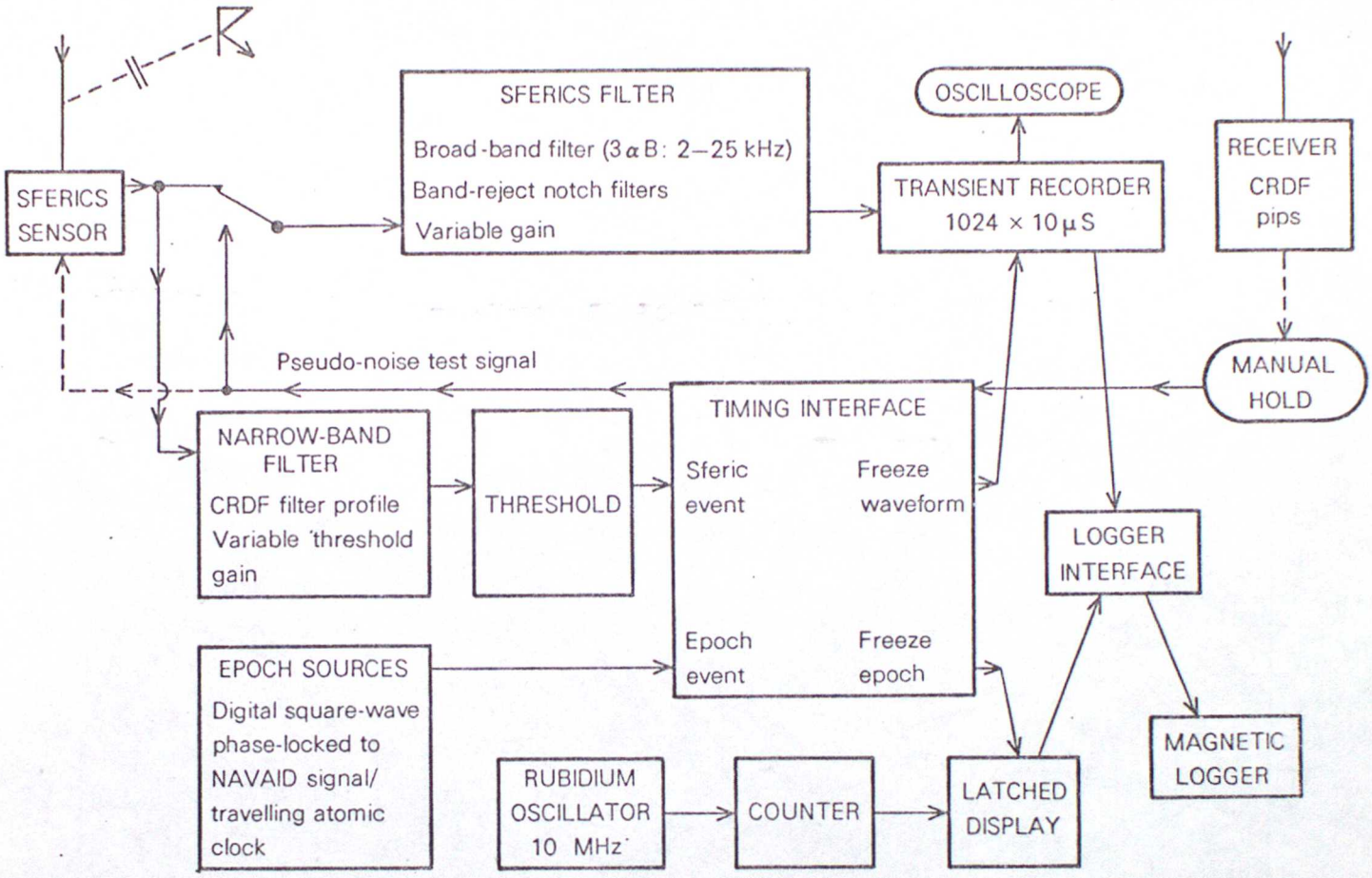

Fig 1: Sferics trial Outstation

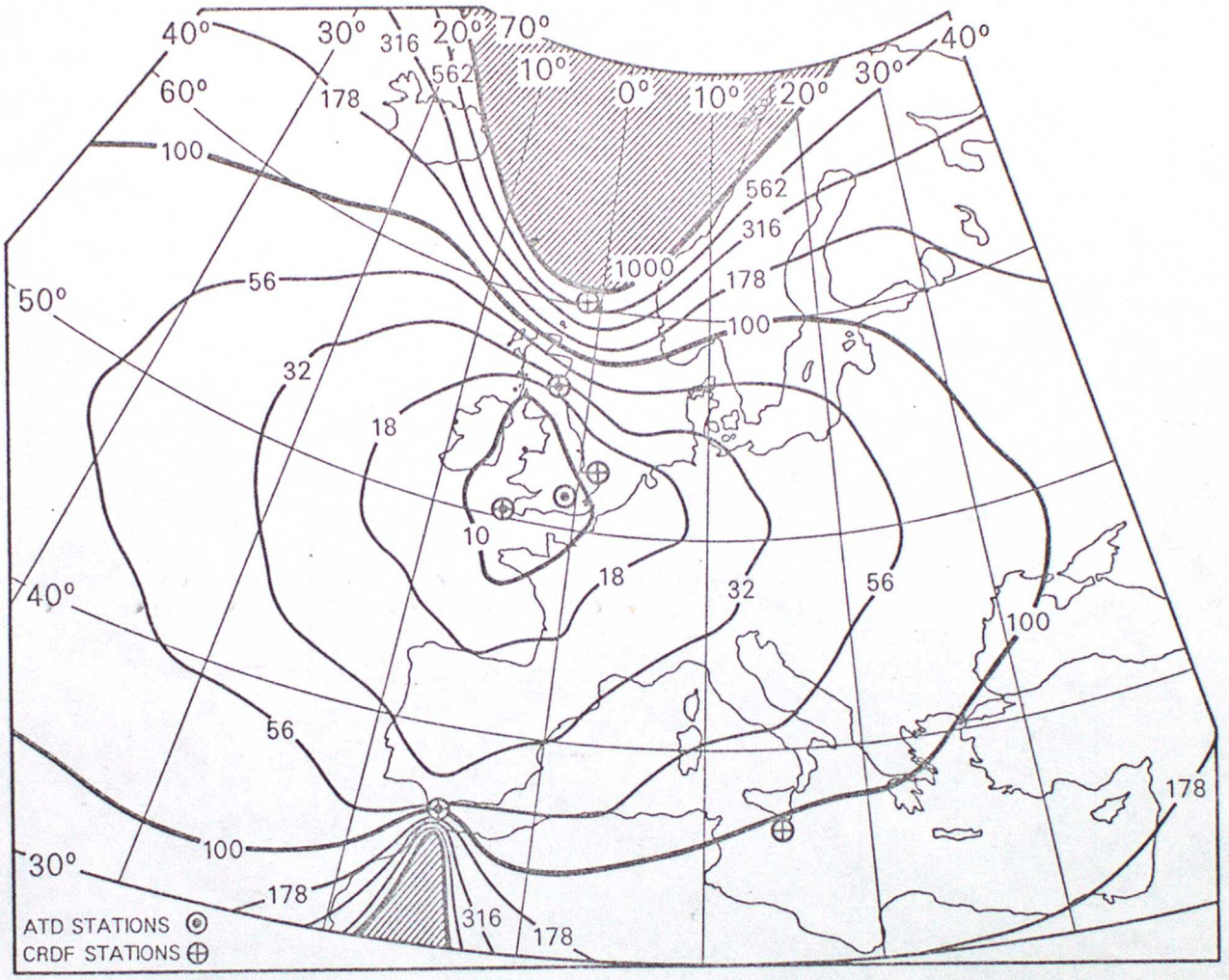

Fig 2: Chart of ATD flash location error (RMS km) assuming 25 μs RMS ATD error. The trial deployment of ATD and CRDF stations is shown.

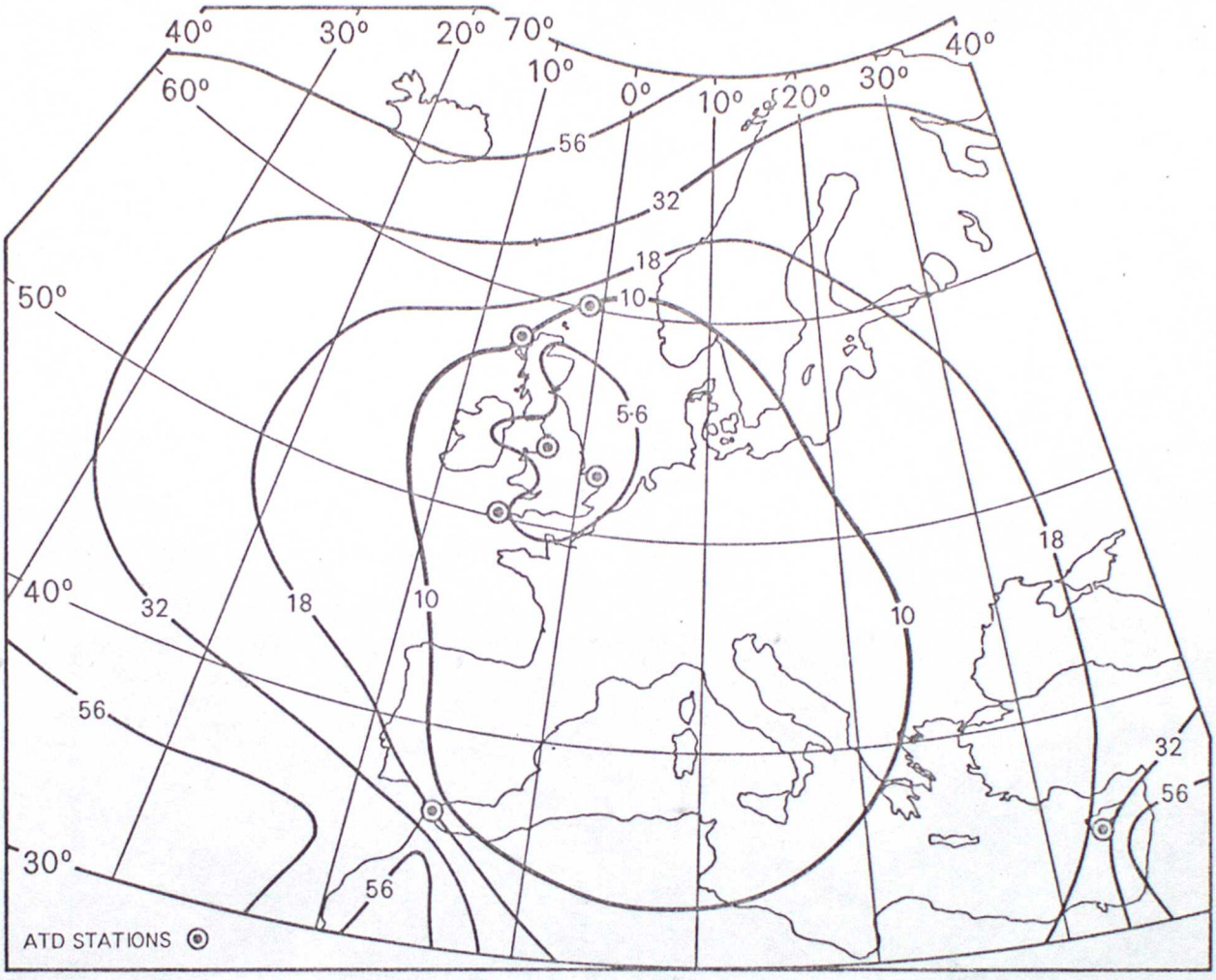

Fig 3: Chart of ATD flash location error (RMS km) assuming 25 μs RMS ATD error, for a possible "operational" network.

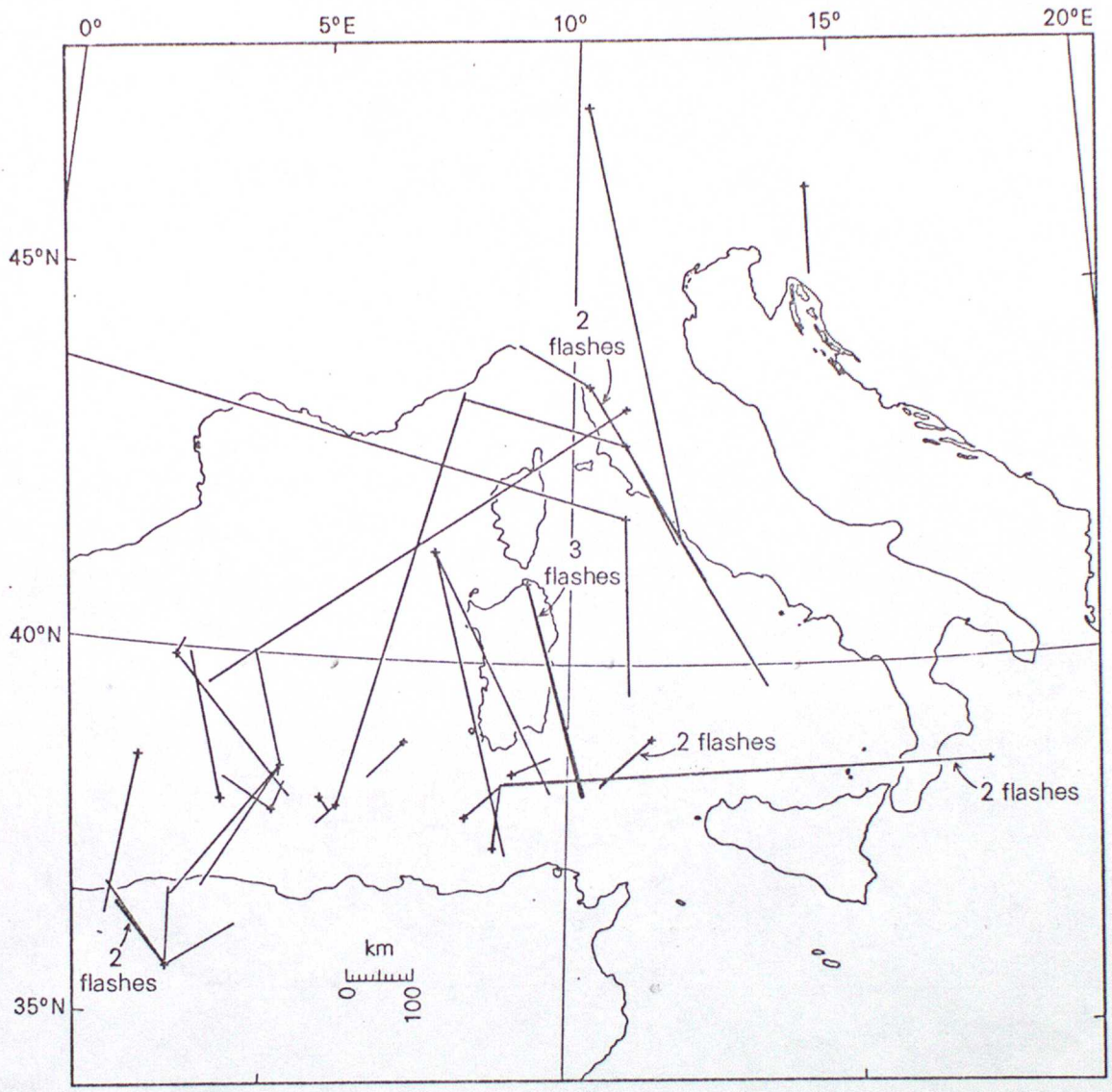

Fig 4: Vectors joining CRDF fixes (+) to the corresponding ATD fixes: Winter conditions.

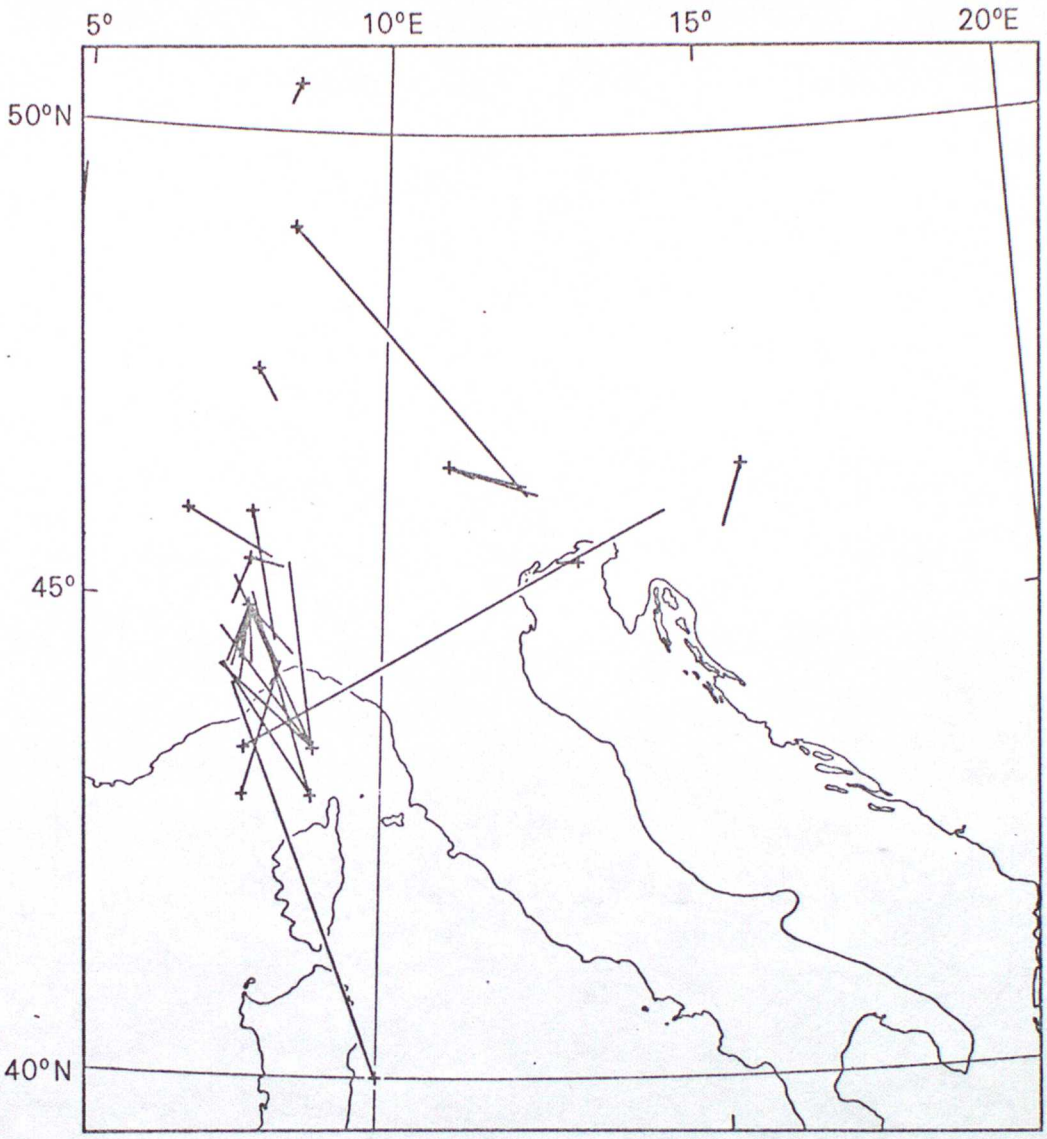

Fig 5: Vectors joining CRDF fixes (+) to the corresponding ATD fixes: Summer conditions.

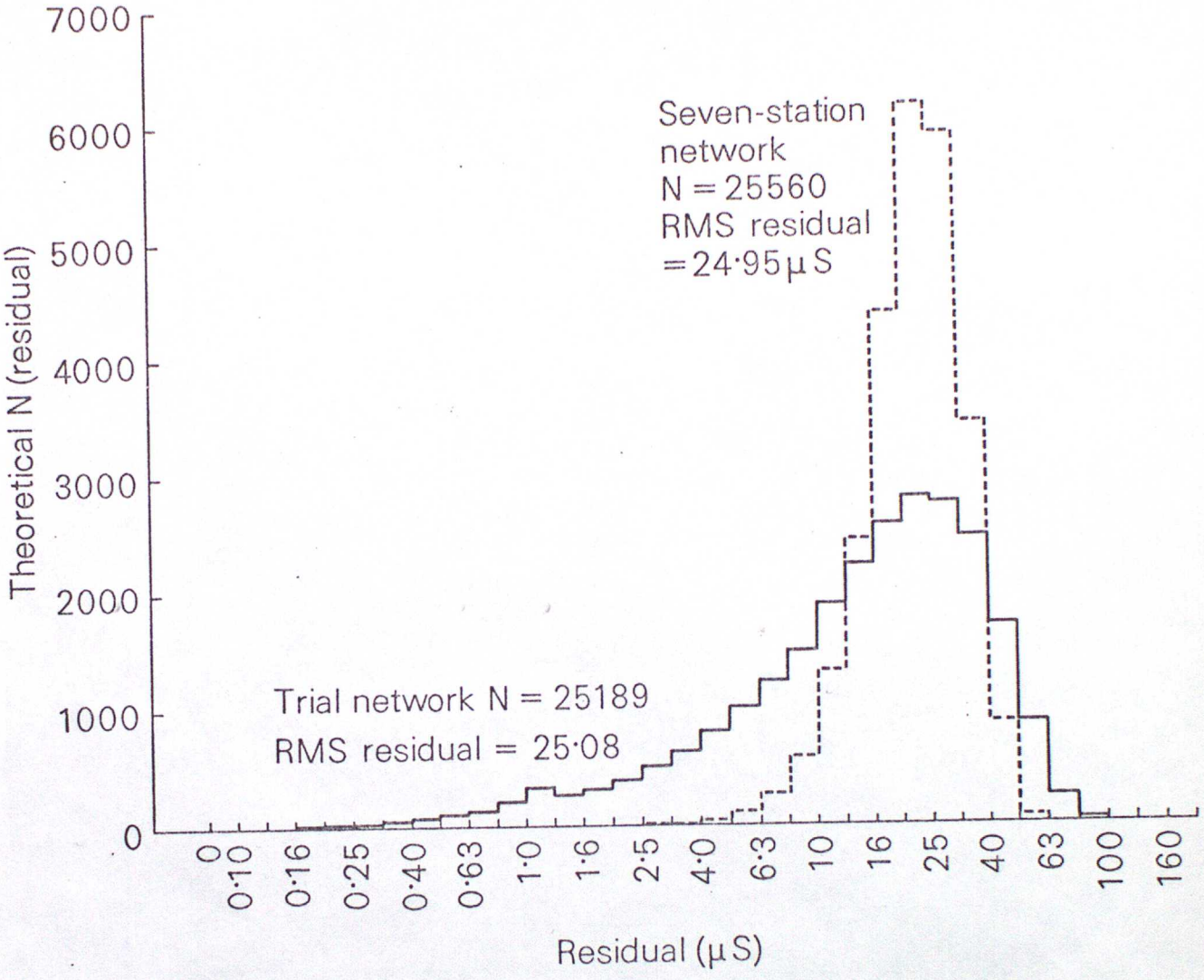

Fig 6: Theoretical histograms showing the distribution of RESIDUAL.

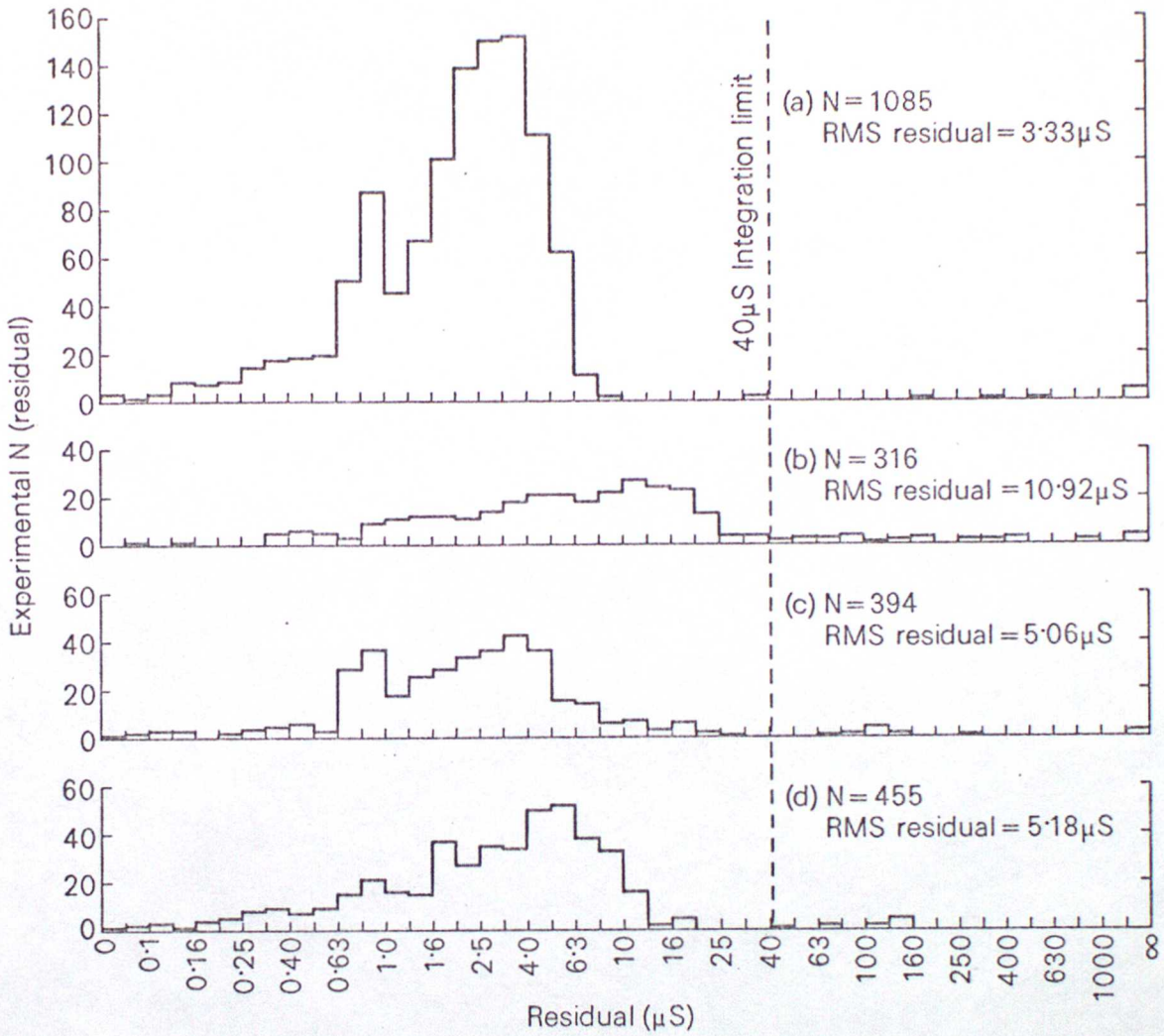

Fig 7: Histograms of RESIDUAL for acceptable trial data fixed between $0^{\circ}N - 80^{\circ}N$, and $80^{\circ}W - 80^{\circ}E$.